

**PhD RESEARCH**  
**Quantitative multi-risk assessment of geomorphological processes:**  
**Application of run-out models to quantify different type**  
**of hazards**



**Byron Quan Luna, ITC**  
**Supervisor: Cees van Westen, ITC**  
**Co-supervisor: Santiago Beguerria, CSIC Zaragoza**  
**Project: Mountain Risk**

# Table of Contents

<b>Introduction</b> .....	p. 5
<b>Research problem</b> .....	p. 5
<b>Research objectives</b> .....	p. 8
<b>Research sub-objectives</b> .....	p. 8
<b>Research questions</b> .....	p.10
<b>1) Quantitative Risk Assessment</b> .....	p.10
1.1) Landslide risk assessment.....	p.10
1.1.1) Runout of landslides in a quantitative risk assessment.....	p.13
1.1.1.1) Factors that influence the run out of landslide.....	p.14
1.1.1.2) Run out models for landslides.....	p.14
1.1.2) Vulnerability to landslides.....	p.17
1.1.3) Risk assessment and risk management for landslides.....	p.17
1.2) Snow avalanche risk assessment.....	p.18
1.2.1) Modeling the snowpack for release area information.....	p.18
1.2.2) Run out models for avalanches.....	p.19
1.2.3) Vulnerability to snow avalanche.....	p.20
1.2.4) Risk assessment.....	p.21
<b>2) Run out numerical modeling</b> .....	p.21
<b>3) Use and extending the application of run out models to estimate new hazard areas</b> .....	p.23
<b>4) Numerical models to be used for rapid mass movements</b> .....	p.24
4.1) One dimensional Voellmy-Salm model.....	p.24
4.2) Two dimensional Voellmy-Salm model.....	p.26
4.3) Voellmy-Salm and frictional with a Lagrangian solution.....	p.28
4.4) Understanding the input parameters in the frictional and Voellmy-Salm model....	p.29
4.4.1) Linear model and non linear models and the need of a turbulent term.....	p.30
4.5) Quadratic model.....	p.32

<b>5) Monte Carlo analysis in a quantitative risk assessment.....</b>	<b>p.33</b>
5.1) Probability density functions, uncertainty and variability.....	p.34
5.2) Application of a Monte Carlo analysis.....	p.35
5.2.1) Defining the statistical distributions of input parameters.....	p.36
5.2.2) Repetition of the model.....	p.36
5.2.3) Outputs of a Monte Carlo Analysis.....	p.36
<b>6) Monte Carlo approach for run out models.....</b>	<b>p.37</b>
6.1) Monte Carlo approach for frictional and Voellmy model.....	p.37
6.1.1) Frictional (Coulomb-like friction) model.....	p.38
6.1.2) Voellmy model.....	p.39
6.2) Monte Carlo approach for quadratic model.....	p.39
<b>7) Field test sites.....</b>	<b>p.41</b>
7.1) Barcelonette basin/Faucon, France.....	p.41
7.1.1) Faucon description and event.....	p.43
7.2) Valtellina valley/Selvetta, Italy.....	p.49
7.2.1) Selvetta debris flow.....	p.53
<b>8) EGU accepted abstracts and future papers.....</b>	<b>p.56</b>
<b>9) Future collaborations.....</b>	<b>p.62</b>
<b>10) References.....</b>	<b>p.63</b>
<b>Appendix.....</b>	<b>p.70</b>

## List of figures

<b>Figure 1.</b> General framework for a quantitative risk assessment using a Stochastic approach for dynamic models.....	p. 7
<b>Figure 2.</b> Framework for landslide risk assessment and management.....	p.11
<b>Figure 3.</b> Energy distribution.....	p.31
<b>Figure 4.</b> Representation of a Monte Carlo analysis for a run out model.....	p.35
<b>Figure 5.</b> Location of the Barcelonette basin.....	p.41
<b>Figure 6.</b> Barcelonette basin and extent of the black marl (gray). Profile of the path of ten torrential stream, morphological sketch and monthly occurrences of events since 1850 Profile of the Barcelonette basin.....	p.42
<b>Figure 7.</b> Flood and Debris flows events occurred in the Barcelonnette basin since 1850 .....	p.43
<b>Figure 8.</b> Morphological map of the Faucon watershed.....	p.44
<b>Figure 9.</b> Check dams built in the Faucon basin.....	p.44
<b>Figure 10.</b> Different view of the Trois Hommes area.....	p.46
<b>Figure 11.</b> View of the Champerousse torrent.....	p.47
<b>Figure 12.</b> House affected by the 2003 Faucon debris flow.....	p.48
<b>Figure 13.</b> Location of the Valtellina Valley.....	p.49
<b>Figure 14.</b> Geological map of the Valtellina valley.....	p.50
<b>Figure 15.</b> View of the Valtellina valley.....	p.50
<b>Figure 16.</b> View of the terraces built in the Valtellina valley flanks.....	p.52
<b>Figure 17.</b> Cumulative rainfall before the Selvetta debris flow (left) and hourly rainfall values measured before the Selvetta event (right).....	p.54
<b>Figure 18.</b> View of the Selvetta debris flow (left). View of the deposits and damage of the event (right).....	p.55
<b>Figure 19.</b> Aerial view of the Selvetta debris flow deposits (left). Contour map containing the trajectory of the Selvetta flow (right).....	p.55

## Introduction

The development of numerical simulation models have increasingly been used for developing risk and hazard maps. Computer models can reduce the time and effort and has the potential to reproduce the phenomenon with consistency. The correct use of these tools can benefit the public authorities when making decisions about communities with potential hazards. The goals of computer modelling should be to assess potential activity in advance with a range of potential scenarios associated with slope failures, debris flows, rock falls and snow avalanches. It is important to evaluate the efficiency and reliability of these simulation tools that integrate the physical models of such events, the numerical methodology and geographical information systems. A variety of models exist for simulating mass-flows and for identifying the hazards that the different phenomena present, a main objective is to evaluate and develop further this models, and find adequate parameters to compare the run-out distances, thicknesses of the deposits in the deposition area, velocities and impact pressures of the flows to measurements observed in the field.

## Research Problem:

Risk can be quantified as the product of vulnerability, cost or amount of the elements at risk and the probability of occurrence of the event with a given magnitude/intensity. The hazard is multiplied with the expected losses for all different types of elements at risk (vulnerability · amount), and this is done for all event types.

$$Risk = \sum (H \sum (VA))$$

Where:

**H:** Hazard expressed as probability of occurrence within a reference period. Hazard is a function of the spatial probability and the temporal probability, related indirectly to some static environmental factors and directly to dynamic factors.

**V:** Physical vulnerability of a particular type of element at risk for a specific type of hazard and for a specific element at risk.

**A:** Amount or cost of the particular elements at risk.

There is a wide variety of dynamic models based on the different rheological models and software that can model the run-out of moving masses. These are able to forecast the propagation of material after failure and to delineate the zone where the elements will suffer a certain impact. The results of these models can be a good input for vulnerability

and risk assessments. Dynamic models may forecast changes in hazard under different scenarios not currently existing. However, most work using these models are based on the calibration of parameters doing a back calculation of past events.

Limited work has been done using these models to quantify the risk derived of the different types of hazards. One of the reasons for this is that it is possible to analyze with some degree of accuracy an event that has already occurred but it is very difficult for larger areas where no event has happened yet.

Run out modeling is rather complicated because of the various physical processes that happens during an event. This processes depends on the initial composition, the characteristics of the path and the material incorporated during the flow. Some of these complex processes are:

- Erosion and entrainment
- Changes in the rheology of flow during one process
- Layering of the flow
- Formation of waves (flow pulses)
- Damming and breaching inside the channels

An approach for quantitative risk assessment is the application of deterministic slope stability models in already mapped susceptible areas, combined with dynamic models. These may provide scenarios of potential hazards under varying conditions. However, many uncertainties are involved in the use of run out models in a quantitative risk assessment:

- Spatial and temporal distribution of the release areas;
- Volume of the release mass;
- Type of movement (release and run-out)
- Probability of the flow reaching an element at risk (velocity, depth and impact pressure)
- Input parameters of the rheological model

These uncertainties problems can be approached using stochastic techniques delivering a spatial and temporal probability of run out patterns (Figure 1)

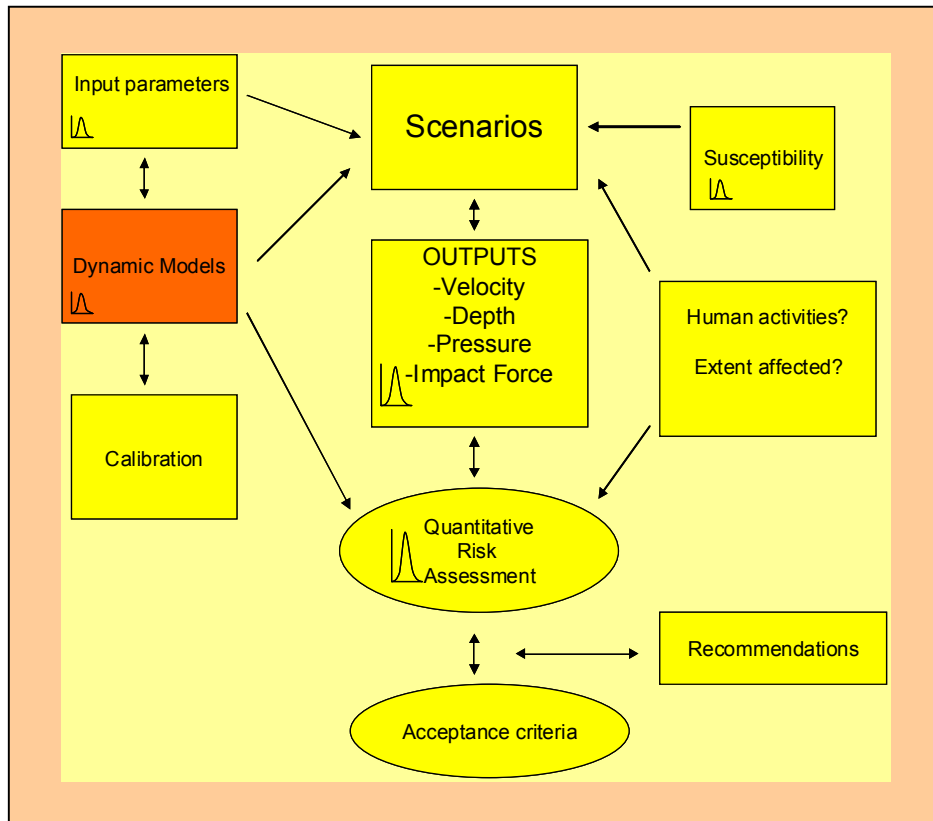


**Figure 1.** General framework for a quantitative risk assessment using a stochastic approach for dynamic models.

The challenge is to determine the rheological behavior of different types of rapid gravity flows based on the morphology, distribution and characteristics of the material deposited along the flow path; to qualify the expected mechanism and apply an appropriate physically based model to simulate the corresponding flows. It is also a challenge to model the exact location of the source areas of debris flows and the spreading of material on the deposition fans.

The desired outputs of modeling for quantitative risk assessment to be coupled with fragility curves:

- Velocities of the flow (maximum and at one point)
- Impact force
- Deposition depth
- Flow height
- Maximum pressures

## **Research Objectives**

The main objective of this research is:

The use and development of techniques for the application of run out models to various hydro-meteorological processes and hazards in a quantitative risk assessment. The main aspect of this research is to employ these proposed techniques to quantify the spatial and temporal probability of the hazard. This will assess the size and impact of the hazard and will be linked with vulnerability and fragility curves. Allowing the generation of risk curves and the combination of the individual risk curves.

## **Research Sub-objectives**

- Benchmark of run out models.

- Identify and contrast the characteristic features of different run out models; the numerical scheme and implementation; and the pre- and post-processing.
- Compare the output results of the different types of models.
- Evaluate the functionality of the models and their proximity to reality.

- Parameterization of run-out models.

- Understand the physical meaning of the different parameters used for run out modeling.
- Perform a sensitivity analysis of the parameters of different models.
- Analyze the influence of the topography and the rheology of the flow in the parameters.
- Evaluate if parameterization can decrease the uncertainties concerning the absolute frequency values and impacts.
- Study the relationship between the parameters and the external factors that influence them.
- Parameterize other types of physical processes to existing models to maximize their performance (e.g. entrainment).

- Validation of models.

- Use of historical data and events to validate the models. Back analysis of the events using dynamical models and calibration of the parameters according to past events.
- Comprehend the simplifications and the assumptions on each model and distinguish their relevance to the type of the event.

- Case studies of use of run-out models for quantitative risk assessment.

- Use precedent risk assessments to examine if run out modeling can assist and in which manner can support a quantitative risk assessment.
- Link output results of modeling with existing and new fragility curves to assess risk.

- Application of results from specific events over larger areas.

- Use of stochastic techniques to decrease the uncertainty in the run out modeling. As result, spatial and temporal probability of run out patterns can be represented.
- Interpolation of results of past events and study areas to new study areas where limited data about landslide event exists.
- Application of the results of research to areas where no events have happened yet and quantify the risk in different types of setting.
- To forecast changes in hazard under different scenarios not currently existing and changes in hazard caused by anthropogenic or natural causes.

## Research questions

- Can run out models be used as a significant tool to quantify risk and how can they be linked inside a risk assessment process?
- Can uncertainties of the models be approached in a stochastic manner?
- Can run out models reproduce the real event in an adequate form?
- How the assumptions made in the models affect the results?
- What does the parameters in the models represents and do they have a physical meaning? How can these parameters be understood and approached inside a risk assessment?
- Can run out models be used where limited data about landslide event has happened?
- Can run out models be used in areas where no event has happened before. How to approach the spatial and temporal probability of this event?

## 1) Quantitative risk assessment

### 1.1) Landslide risk assessment

Landslides, defined as the movement of a mass of rock, debris or earth down a slope (Cruden, 1991), can be triggered by a variety of external factors, such as intense rainfall, earthquake shaking, water level change, or rapid stream erosion that cause an increase in shear stress or decrease in shear strength of slope-forming materials. In addition, human activities such as deforestation or excavation of slopes for road cuts and building sites have become important triggers for landslide occurrence.

Recent advances in risk analysis and risk assessment are beginning to provide systematic processes to formalize slope engineering practice and enhance slope management (Fell and Hartford, 1997). In recent years, risk analysis and assessment has become an important tool in addressing uncertainty inherent in landslide hazards.

Landslide risk assessment involves the estimation of the level of risk, deciding whether or not it is acceptable, and exercising appropriate control measures to reduce the risk when the risk level cannot be accepted (Ho et al., 2000). It requires the following issues to be addressed: (a) probability of landsliding, (b) run out behavior of landslide debris, (c)

vulnerability of property and people to landslide, (d) landslide risk to property and people, and (e) management strategies and decision-making (Fig. 2).

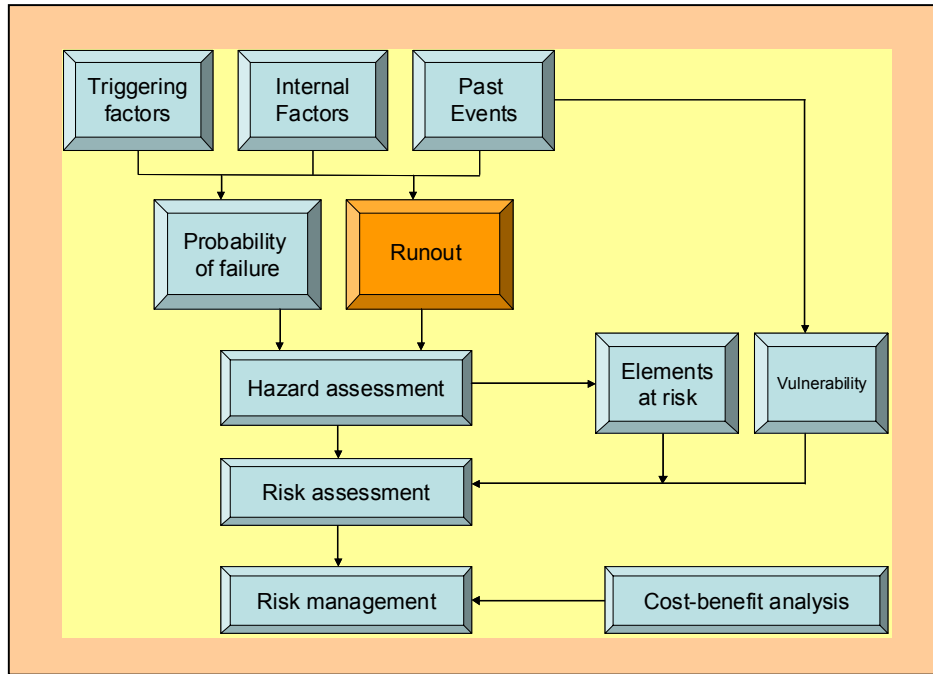


**Figure 2.** Framework for landslide risk assessment and management.

In terms of probability, landslide risk when defined as the annual probability of loss of life of a specific individual may be calculated as follows (Morgan et al., 1992):

$$R(I)=P(H)\times P(S|H)\times P(T|S)\times V(L|T) \quad (1.1)$$

where R (DI) is the risk (annual probability of loss of life to an individual); P (H) is the annual probability of the landslide event; P (S|H) is the probability of spatial impact given the event; P (T|S) is the probability of temporal impact given the spatial impact; and V (L|T) is the vulnerability of the individual (probability of loss of life of the individual given impact).

For a case involving property damage the equivalent expression would be

$$R(P)=P(H)\times P(S|H)\times V(P|S)\times E \quad (1.2)$$

where  $R(PD)$  is the risk (annual loss of property value);  $P(H)$  is the annual probability of the landslide event;  $P(S|H)$  is the probability of spatial impact;  $V(P|S)$  is the vulnerability of the property (proportion of property value lost);  $E$  is the element at risk (the value of the property).

When assessing the probability within a specified period of time and within a given area, recognizing the conditions that caused the slope to become unstable and the processes that triggered the movement is very important. The factors which determine the probability for a particular slope can be grouped into two categories: (1) the internal factors which make the slope susceptible to failure such as geology, slope gradient and aspect, elevation, soil geotechnical properties, vegetation cover and long-term drainage patterns and weathering; and (2) the triggering factors which change the slope from stable to an unstable state and initiate a failure in an area of given susceptibility such as heavy rainfall and earthquakes.

Probability depends on both the internal and triggering factors. If the triggering factors are not taken into account, the term “susceptibility” may be employed to define the likelihood of occurrence of a landslide event. Different methods have been developed to calculate the probability of a landslide.

On a regional scale various methods have been developed to assess the probability of a landslide. Soeters and van Westen (1996) and van Westen et al. (1997) divided these methods into inventory, heuristic, statistical, and deterministic approaches.

The most used and forward initial approach to study landslide hazard is the compilation of a landslide past events with an inventory. Such inventories are the basis of most susceptibility mapping techniques. On detailed landslide inventory, the basic information for landslide hazards or risk level should be provided, including the state of activity, identification, dominant type of movement, primary direction of movement, estimated thickness of material, and date of known activity for each landslide (Wieczorek, 1984). The triggering and frequency–magnitude relations that help understand landslide probabilities may be derived from landslide inventories of past events.

In the heuristic approach, expert opinions are used to estimate landslide potential from data on preparatory variables. They are based on the assumption that the relationships between landslide susceptibility and the preparatory variables are known and are specified in the models

Deterministic approaches are based on slope stability analyses. They have been widely used to assess landslide probability in detailed areas. The advantage of the deterministic models is that they permit quantitative factors of safety to be calculated with due consideration for the variability of soil properties if necessary,

Statistical models involve the statistical determination of the combinations of variables that have led to landslide occurrence in the past.

For site-specific slopes, the probability of failure is usually considered as simply the probability that the factor of safety is less than unity. The performance function of slopes, denoted by  $G(X)$  where  $X$  is the collection of random input parameters, is a function which defines the failure or safety state of a slope. The function is defined that failure is implied when  $G(X) < 0$  and safety by  $G(X) > 0$ . The boundary defined by  $G(X) = 0$  separating the safety and failure domains is called the limit state boundary.

The performance function for a slope is usually taken as

$$G(X) = R(X) - S(X) \quad (1.3)$$

This function has a lower degree of non-linearity (Mostyn and Fell, 1997). The performance function of a slope is usually formulated using the simplified limit equilibrium method, such as the ordinary method of slices, simplified Bishop's method, and simplified Janbu's method.

Once the performance function is defined, the probability of failure of a slope can be estimated by the following methods:

(1) The first-order-second-moment (FOSM) method. This method characterizes the frequency distribution of the factor of safety  $F$  in terms of its mean value  $\mu_F$  and standard deviation  $\sigma_F$ . The reliability index  $\beta$  is computed from  $\beta = (\mu_F - 1.0) / \sigma_F$ . The reliability index is regarded as an index of the degree of uncertainty and it can be related to the probability of failure if the frequency distribution is known.

(2) Monte Carlo simulation. This method involves a computerized sampling procedure used to approximate the probability distribution of the factor of safety by repeating the analysis many times; especially the target reliability to be evaluated is small. A set of random numbers is generated for the random variables according to the chosen frequency distributions of the input parameters.

### **1.1.1) Runout of landslides in a Quantitative Risk assessment**

To know the extent of the endangered area is very important to landslide risk assessment. These require accurate prediction of the run out behavior of a landslide, such as how far and how fast will a landslide travel. The run out behavior is a set of quantitative spatially distributed parameters that define a landslide. These parameters for the purpose of landslide risk assessment mainly include (Hung, 1995):

- Run out distance;
- Run out width;
- Velocity;

- Pressure
- Depth of the moving mass;
- Depth of deposits.

#### **1.1.1.1) F actors that influence the run out of landslides**

##### - Slope characteristics:

This includes slope geometry, the nature of the slope forming material, and upslope influence zone. The motion behavior of the sliding material involves the redistribution of the potential energy available at failure into friction energy, disaggregating or remolding energy, and kinetic energy. Leroueil et al. (1996) and Leroueil and Locat (1998) examine the relationship between the nature of the slope forming material and slope movements.

##### - Modes of movement and mechanism of failure

Loose granular soils tend to collapse when sheared, which under undrained condition results in an increase in pore water pressure. Consequently, failures in contractive soils often evolve into debris flows that may travel great distances because even minor strain may cause liquefaction. Dilatant soils expand upon shearing and a continued influx of water is required to sustain their mobilization. Consequently, failures in dilatant soils tend to be relatively slow-moving slides, depending on the availability of rainfall amount and intensity and soil permeability (Fleming et al., 1989). Once a landslide mobilizes, the modes of movement, disintegration of the failure area during motion and convergence of surface runoff obviously influence flow velocity and travel distance. The availability of water further affects whether it assumes characteristics typical of debris flows, hyperconcentrated flows, or sediment-laden floodwaters.

##### - Flow path

The characteristics of the path can affect the mode of the movement. Is very important the gradient of the path, the possibility of channelization, the ground surface on which the flow travels, type of vegetation, extent of catchment which collects surface water and discharges into the down slope area.

#### **1.1.1.2) Run out models for landslides**

A variety of techniques have been developed to assess the travel distance and the velocity of a flow. It should be understood that the movement of a flow is complex and more than one phenomenon may be operating at the same time, and different phenomena may prevail at different locations of a given even

#### - Empirical models

Empirical methods include mass-change method and the angle of reach. The mass-change method is based on the phenomenon that as the landslide debris moves down slope, the initial volume/mass of the landslide is being modified through loss or deposition of materials, and that the landslide debris halts when the volume of the actively moving debris becomes negligible (Cannon and Savage, 1988). The average mass/volume-change rate of landslide debris was established by dividing the volume of mobilized material from the landslide by the length of the debris trail.

Another empirical approach is the angle of reach, defined as the angle of the line connecting the crest of the landslide source to the distal margin of the displaced mass. Corominas (1996) conducted a detailed study on the influence of various factors that affect the angle of reach using landslide records, and showed a linear correlation between volume and angle of reach for all types of failures. Regression equations for calculating the angle of reach of each landslide type were developed. Earth flows have the highest mobility, and rockfalls have the lowest mobility. A common problem with the angle of reach method is that the scatter of the data is too large to permit reliable use for any but the most preliminary predictions of the travel distance.

Empirical methods are generally simple and relatively easy to use; the information required by these methods is usually general and readily available.

#### - Analytical models based on energy considerations

The analytical methods include different formulations based on lumped mass approaches in which the debris mass is assumed as a single point. The simplest type of analytical methods is the sled model (Sassa, 1988), which assumes that all energy loss during debris movement is due to friction and describes the landslide as a dimensionless body moving down the profile of the path. The movement is controlled by a single force resultant, representing the gravity driving force as well as all movement resistance. The ratio of the vertical to horizontal displacement of the center of gravity of the block equals the friction coefficient used in the analysis. This method can provide an effective means for the calculation of run out distance, velocity and acceleration of debris movement. Sassa (1988) improved the sled model by considering the effect of pore fluid pressures at the sliding plane. He considered the frictional resistance along the sliding plane to be a function of the internal friction angle and the pore pressure coefficient,  $B$ . The apparent friction angle in the improved sled model can be expressed as the combined effects of the internal friction angle of debris material, and the motion-induced pore pressure.

Hutchinson (1986) developed a model for the prediction of run out distances of flows in loose, cohesionless materials by assuming that the shape of a debris flow is a uniformly spread out sheet. In the model, the basal resistance of the debris mass is assumed to be purely frictional, and the excessive fluid pressure in the debris mass is assumed to be dissipating according to the one-dimensional consolidation theory. As debris moves downslope, the shear resistance on the sliding plane increases due to a dissipation of

excessive pore pressure. The debris mass halts when the resultant force along the sliding plane becomes zero.

The frictional and turbulent model by Voellmy is also based on a lumped mass approach. The lumped mass cannot account for lateral confinement and spreading of the flow and the resulting changes in flow depth. To apply these methods, some specific parameters are required, such as pore pressure parameters and debris thickness, relation of residual strength with shear rate.

Many of the analytical approaches can also be extended to provide an estimate of the velocity profile and acceleration of the landslide, in the case of real time solution techniques (Hung, 1995), the travel time of the flow. Observation of the superelevation of the flow around the bends and run-up of the flow against an obstacle also allow an estimate of the velocity to be made. This alternative approach provides an independent method to determine the velocity at certain point and may serve as a check of the predictions by analytical models.

#### - Numerical models

Numerical methods for modeling run out behavior of landslide debris mainly include fluid mechanics models and distinct element method. Continuum fluid mechanics models utilize the conservation equations of mass, momentum and energy that describe the dynamic motion of debris, and a rheological model to describe the material behavior of debris. By solving a set of governing equations with a selected rheological model describing the flow properties of the debris, the velocity, acceleration and run out distance of debris can be predicted (Cheng, 2000). Hung (1995) developed a modified continuum model. The method is different from the classical continuum fluid mechanics modeling methods discussed above. In his model, debris mass is discretized into column elements, and the rheological properties of debris at the sliding plane are accounted for. The longitudinal rigidity of the flowing mass is considered in conjunction with the lateral earth pressure coefficient. The friction resistance is assumed to act only at the base of the sliding plane. Pore pressure effects are incorporated with the pore pressure coefficient—the ratio of pore pressure to the total normal stress at the base of the column element. The friction angle can be assumed to be a function of displacement to simulate shear strength decays from peak to residual. The pore pressure coefficient can be expressed as a function of location or elapsed time to simulate drainage and consolidation effects. This method is easy to use, and the debris movements at different time intervals can be simulated.

Rheological models have to be selected, and the required rheological parameters have to be determined by back-analysis from the landslide cases. After determining the probability of landsliding and the areal extent that would be potentially affected by the landslide, landslide hazard can be delimited, and elements at risk can be defined.

### **1.1.2) Vulnerability to landslides**

Vulnerability is defined as the level of potential damage, or degree of loss, of a given element (expressed on a scale of 0 to 1) subjected to a landslide of a given intensity (Fell, 1997). Vulnerability assessment involves the understanding of the interaction between a given landslide and the affected elements. Generally, the vulnerability to a landslide may depend on (a) run out distance; (b) the volume and velocity of sliding; and (c) the elements at risk, their nature and their proximity to the slide. The vulnerability of lives and property to a landslide may be different. For example, a house may have similar and high vulnerability to a slow-moving and a rapid landslide, but persons living in the property may have a low vulnerability to the slow-moving landslide but a higher vulnerability to the rapid landslide (Fell, 1997).

The assessment of vulnerability is somewhat subjective and largely based on historic records. For example, the vulnerability of a house immediately at the base of a steep slope down which a debris flow may occur is clearly higher than for a house at the limits of deposition area (because the velocity of flow is much less) (Fell, 1997).

### **1.1.3) Risk assessment and risk management for landslides**

Once the probability of landsliding, the run out of landslide debris, elements at risk, and vulnerability terms have been derived, risk values may be simply obtained by using the risk formula (1.1) and (1.2). Different types of analysis can be used to quantify the risk from the potential failure. The procedure consists of the following steps (Wu et al., 1996):

- Examine possible triggering factors, such as earthquakes or/and rainfall;
- Identify possible failure modes;
- Estimate probability of failure for each failure mode;
- Evaluate run out behavior of landslide for each failure mode;
- Assess the risk for each failure mode; and
- Sum the risk for all possible failure modes

Once the risk from a landslide is identified, measures may be taken to mitigate the risk to the community if necessary. The community faced with a landslide has a variety of strategies to deal with it, and these strategies may be grouped into planning control, engineering solution, acceptance, and monitoring and warning systems. Planning control may be seen as reducing expected elements at risk; the engineering solution strategy as reducing either the probability of a landslide or the probability of spatial impact of a landslide; the acceptance strategy as acceptable or unavoidable; and the monitoring and warning system strategy as reducing expected elements at risk by evacuation in advance of failure.

## **1.2) Snow avalanche risk assessment**

Snow avalanches are an important type of hazard in mountainous terrain. Quantitative risk assessment is recognised to be a good basis for land use planning in avalanche prone areas. An important feature of an effective risk calculation procedure is its adaptability to territory changes, both in the release zone and in the run-out area.

As in a “landslide quantitative risk assessment”, the risk is a function of hazard,  $H$ , vulnerability,  $V$ , and element at risk,  $E$ . For a given element at risk, the specific risk is defined as the product of hazard and vulnerability:

For a generic point on an avalanche path, hazard is defined as the probability that an avalanche, with a particular intensity reaches the point within a given time.

In order to calculate risk, and consequently to evaluate the direct effect of avalanches on exposed elements, avalanche intensity is usually described in terms of impact pressure, according to Wilhelm (1998) and Keylock and Barbolini (2001). Impact pressure in any generic point of the avalanche path can be obtained by the use of a dynamical avalanche simulation model. The dynamics model gives as an output, the dynamical avalanche parameters in space and time, such as velocity, flow depth and impact pressure.

A probability density function of the release area (depth and length); can be determined from statistical analysis of snowfall data, assuming the release depth is a function of the three-day snow precipitation (Salm, 2004). Other types of approaches to find release areas are similar to the ones used for landslides with the difference that the packing of the snow and some meteorological aspects are taken into account (solar radiation, wind, temperature).

### **1.2.1) Modeling the snow pack for release area information**

A comprehensive model for the snow cover should include information of the underlying soil and drifting snow (Lehning et al., 1999). It is important to understand the evolution of the snow cover based on meteorological input data.

Parameterization of the snow microstructure, allows a detailed representation of the layered snow structure. The following individual processes should be modeled:

- Heat Transfer
- Settling
- Phase Change
- Water Transport
- Metamorphism

## 1.2.2) Run out models for avalanches

The damage an avalanche causes will be a function of the pressure exerted by the avalanche upon the structure in the run out zone. Because impact pressure is a function of velocity it is necessary to obtain the avalanche velocity as a function of position throughout the run out zone to estimate the degree of damage that will be caused. Avalanche dynamic models can be used to obtain the run out zone velocity profiles. A great number of models have been proposed for modeling the motion of a snow avalanche, with a big variability due to the complexity of avalanche dynamics and the lack of detailed knowledge of flowing snow (Harbitz, 1999).

It is important to have in mind that all avalanche-dynamics models make great simplifications to solve for the flow velocity. Models using forms of a friction law are currently employed for avalanche zoning in Austria, Iceland, Italy, and Switzerland.

### - Statistical methods

These methods require accurate knowledge of past avalanche run out to calculate avalanche boundaries. The two main statistical models used in practice are the one developed by Lied and Bakkehoi and the one developed subsequently by McClung and Lied. Both attempt to predict the extension of the long-return period avalanche for a given avalanche path with a return period of approximately 100 year. All these methods are based on the correlations existing between the run out distance and some topographic parameters.

Many extensions of the early model developed by Lied and Bakkehoi have been proposed over the last twenty years either to tune the model parameters to a given mountainous region or adapt the computations to other standards. For instance, other topographic parameters such as the inclination of the starting zone or the height difference between the starting and deposition zones.

Although statistical methods have been extensively used throughout the world and have given fairly reliable and objective results, many cases exist in which their estimates are wrong. Such shortcomings are due to the fact that for some avalanche paths, the dynamic behavior of avalanches cannot be merely related or governed by topographic features.

### - Dynamic models

This involves quantifying the basic mechanisms affecting the avalanche motion. Avalanches can be considered at different scales: large, intermediate and small scale.

The larger scale, leads to the simplest models. The main parameters include the location of the gravity centre and its velocity. Mechanical behavior is mainly determined by the friction force applied by and to the bottom of the avalanche. This models dates back to the beginning of the 20th century. The Voellmy-Salm-Gubler (VSG) model and the Perla-Cheng-McClung model are probably the best-known avalanche-dynamics models

used throughout the world. In this model, a flowing avalanche is considered as a sliding block subject to a friction force. This model enables us to easily compute the run out distance, the maximum velocities reached by the avalanche on various segments of the path, the flow depth (by assuming that the mass flow rate is constant), and the impact pressure.

Less advanced models (intermediate) have also been developed. They benefit from being less complex than three-dimensional numerical models and yet more accurate than simple ones. Such models are generally obtained by integrating the motion equations across the flow depth in a way similar to what is done in hydraulics for shallow-water equations. It is possible to compute the spreading of avalanches in their run out zone or relate parameters used in the models to the rheological properties of snow. Considerable progress in the development of numerical depth-averaged models has been made possible thanks to the increase in computer power and breakthrough in the numerical treatment of hyperbolic partial differential equation systems.

### **1.2.3) Vulnerability to snow avalanches**

Research concerning vulnerability relations for use in snow avalanches risk assessment are quite recent ([Wilhelm, 1998], [Jónasson et al., 1999], [Barbolini et al., 2004a] and [Barbolini et al., 2004b]) and mainly refers to the vulnerability of buildings and people exposed to avalanche action. The only relations for buildings subject to dense flow avalanches are provided by Wilhelm (1998). Analyzing the effect of avalanches on about fifty buildings on the Swiss territory affected by dense avalanches, he proposed five different curves, according to different building categories, relating vulnerability, expressed as the ratio between the cost of repair and the building value, to avalanche impact pressure.

Jónasson et al. (1999), proposed a vulnerability relation that gives the survival probability for a person inside a building affected by a dense avalanche as a function of avalanche velocity. Concerning powder avalanches the only available vulnerability relations in literature are those presented by Barbolini et al. (2004), obtained from analysis of two Austrian catastrophic avalanches data, which gives the vulnerability for buildings and the death probability for a person inside them as functions of avalanche impact pressure.

The majority of the relations show a similar trend. Vulnerability remains zero as long as avalanche intensity is lower than a first threshold, which can correspond to the first visible damages to elements exposed. After the first threshold vulnerability remains constant until it reaches a second threshold which corresponds to the first structural damages to buildings and consequently the safety of people inside them is compromised. Then it increases (usually linearly) until it reaches an upper intensity threshold, representing the complete loss. For avalanche intensities greater than the upper threshold, vulnerability remains equal to one, since no more damages can be produced to the exposed element.

### **1.2.4) Risk assessment for snow avalanches**

Once the probability of occurrence for an avalanche to be triggered, the run out behavior and the vulnerability terms have been derived, risk values may be obtained by using the risk formula.

## **2) RUN OUT NUMERICAL MODELLING**

Understanding, forecasting and controlling the hazard associated with geomorphological processes is still an empirical task. It involves qualitative and quantitative analyses, including model simulations, from various disciplines (geomorphology, structural geology, engineering geology, hydrology, hydrogeology, geophysics, geotechnics, and civil engineering). Analysis can be performed at several spatial and temporal scales according to the objective of the hazard assessment (van Westen et al., 2006). Accordingly, the methods and tools used for the analysis are very different; empirical or statistical techniques are generally applied to predict susceptibility at regional scale, more process-based approaches are applied at the local scale.

A very important part of any hazard risk assessment is a quantitative estimate of post-failure motion defining distance, material spreading and velocity. Some slope movements are slow and ductile, other slope movements are brittle and after a certain slow deformation or sudden loading, they accelerate and potentially fluidize. The main aspect of run out modeling is to reproduce accurately the dynamics the geomorphologic processes and to reliable forecast of the potential transformation and hazard.

Post-failure movement is controlled by a complex interaction between mechanical and fluid properties that reflects spatio-temporal trends in the effective strength and rheological properties of the material (Vulliet, 2000). Slope movements are not rigid moving bodies and zones of compression and extension will be generated caused by heterogeneity of the moving pattern. In landslides, this will create undrained loading effects leading to the generation of excess pore pressure and in snow this will create a fluidize layer.

Because of the complex interactions during the flow phase, the parameterization of hydrological and geomechanical factors by field and laboratory tests is not sufficient to describe the post-failure movement patterns (Vulliet, 2001) and not all the processes can be included in detail in the simulation.

Several methods have been developed to analyze their travel distance and velocities, ranging from empirical methods to physically-based approaches. Empirical methods are based on field observations and on the analysis of the relationships between parameters characterizing the travel path (local morphology), the mass volume and the run-out distance. Simple statistical analyses can be used to produce indexes expressing, directly or indirectly, the mobility of the mass. Analyses of relevant datasets with a geometrical

approach (Corominas, 1996; Finlay et al., 1999) have proposed that the angle of reach may be taken as the measure of the relative mobility or as the coefficient of friction of a sliding body (Scheidegger, 1973). There are large controversies on the interpretation of the volume dependence to the angle of reach (Davies et al., 1999; Hunter and Fell, 2003). These methods require comprehensive datasets with the identification of both source point and end point. However, the underlying distributions are not specified and may reveal large scatter (van Westen et al., 2006) and they are not able to provide an estimate of the flow velocities, which is important to evaluate the vulnerability of infrastructures and buildings and their occupants.

Physically-based models, most of them solved numerically, model the movement using constitutive laws of solid and fluid mechanics. Three main groups of models have been developed (Hung, 1995): lumped-mass approach, 2-D models looking at a typical velocity profile of the moving mass, and 3-D models treating the flow over irregular topographic terrains. Most models are simplified by integrating the internal stresses in either vertical or bed-normal directions to obtain a form of Saint-Venant or Navier-Stokes equations (*shallow water assumption*) (Iverson, 2005). Derivations of the constitutive relationships using the theory of frictional grain flow (Savage and Hutter, 1991; Hutter et al., 1995) or the theory of mixture flow (Iverson, 1997; Denlinger and Iverson, 2004; Iverson et al., 2004). A review of these methods has been recently presented by Hung et al. (2005) and Harbitz (1999). To simulate one-phase constant-density flows, most models use the semi-empirical approach called “equivalent fluid method” introduced by Hung (1995) assigning simple constitutive relationships judged appropriate for a given material. The rheologies used in most models are the frictional-turbulent Voellmy resistance relationship (proposed initially for snow avalanches) and applicable for granular cohesionless material with or without the presence of a pore fluid, and the viscoplastic Bingham (or Herschel-Bulkey) resistance relationship applicable for fine plastic clay-rich material (Soussa and Voight, 1991; Laigle and Coussot, 1997). More complex rheologies have also been proposed such as the Coulomb-viscous model (Johnson and Rodine, 1984), the bi-linear constitutive equation (Locat, 1997), the generalized viscoplastic equation (Chen, 1988), and a dilatant rheology for modeling the run-out of mudflows (Takahashi, 1991).

Under the shallow water assumption, 2-D and 3-D solutions of fast gravitational flows can be derived from the momentum equation for unsteady fluid flow, evaluating the dynamic equilibrium for a single column isolated from the flowing mass and integrating the stresses in the bed-normal or vertical direction. Several forces diagrams can be used to solve the equilibrium of the column (Iverson, 2005). Eulerian and Lagrangian solutions of these governing equations have been developed (Hung, 1995). Non-hydrostatic internal tangential stress has been introduced by Savage and Hutter (1991) and Hutter et al. (1995) assuming that the moving mass is frictional and undergoes plastic deformation. Another approach is the generalization of the Savage-Hutter theory, proposed by Iverson (1997) and based on grain-fluid mixture theory to account explicitly for viscous pore fluid effects. 3-D solutions have also been developed using Eulerian schemes implemented on fixed rectangular grids. These fluid dynamic models need to consider fluid discharges (and associated momentum fluxes) across the domain and its boundaries.

Flo-2D (O'Brien et al., 1993) is one of the few existing models that have been used on real cases, and for practical work (Garcia et al., 2003). 3-D solutions assuming non-hydrostatic lateral stresses have been developed recently (Gray et al., 1999; McDougall and Hungr, 2004) especially to take into account of the bed-parallel strain in the flow and to provide realistic simulation of the internal stress state. A 3-D kinetic scheme incorporated in an unstructured finite-volume mesh have been proposed by Mangeney-Castelnau et al. (2003) to solve the 3D Savage-Hutter equations, and modified by Pirulli (2005) to account for irregular terrain. Alternative solution has also been investigated such as coupling the numerical methods of Cellular Automata and Smoothed Particle Hydrodynamics or using variable time steps.

The development of these techniques needs detailed topographic information on both the travel paths and the deposition areas. This constitutes a problem because of the lack of accuracy in the available DEM's and the changes in topography during depositional process. However, major improvements can be expected from airborne laser scanning techniques, such as LIDAR, which will be beneficial for many aspects of landslide hazard modeling (Glenn et al., 2006).

Estimates of run-out distance are associated to relevant estimates of initial volumes of failed material. However, other processes may be involved in development of fast gravitational flows. Material accumulated in gullies in the source areas can be entrained by the flow and can be added to the total mass. Scouring of the bed material during the flow event in the run out track is also of big importance (Hungr et al., 1984; Chen, 1987; Jakob et al., 2000; Hungr and Evans, 2004) and entrainment capabilities have to be included in the numerical models for instance through erosion/deposition rate formulas.

### **3) Use and extending the application of run out models to estimate new hazard areas.**

Many statistical techniques have been developed and applied to landslide susceptibility assessment and mapping. (Carrara et al., 1991; Fabbri and Chung, 1996; Guzzetti et al., 1999). Such techniques are capable to predict the spatial distribution of landslides adequately with a relatively small number of conditioning variables (Coe et al., 2004). However, these techniques lack the ability to evaluate temporal probabilities and long-term changes in landslide activity.

A particular problem to the application of time-dependent assessments is that most records cover only a short period (Glade et al., 2001) and a small geographical area (Chung and Fabbri, 1999). Scarcity of supporting temporal information on the meteorological or seismic triggering events prevents the definition of reliable magnitude-frequency curves at the regional scale (Guthrie and Evans, 2005). Moreover, records do seldom contain information on the date of occurrence, the volume mobilized or even the

type of movement (Hungri et al., 1999; Coe et al., 2003) and different landslide types are merged into one large dataset which hides the influence of different controlling factors (van Westen et al., 2006).

Therefore, the challenge is to add a temporal dimension, as well as information on the magnitude of events, to the already available susceptibility assessments in order to produce real hazard maps. The use of deterministic (physically-based) methods (Dietrich et al., 2001; Chen and Lee, 2003; Savage et al., 2003) in combination with probabilistic statistical techniques should theoretically be able to overcome these problems and complement any spatial and historical databases that are already available. To forecast landslide hazard outside the boundaries of existing active landslides, simulations based on probabilistic models as well as event-tree methods (Hsi and Fell, 2005) are the tools to be used to extend the knowledge gained at the local scale to a larger area and to obtain occurrence probabilities and magnitudes for different types of slope movements (Aleotti and Chowdhury, 1999; Wong, 2005).

When information on the temporal distribution of landslides is scarce, information on the spatio-temporal occurrence of landslides and on possible trends in the process activity under changing environmental conditions should be obtained by probabilistic, physically based modeling. This provides an opportunity to investigate run-out frequencies and magnitudes of landslides in the absence of documentation of former events (volume involved, landslide travel distances).

## 4) Numerical models to be used for rapid mass movements

### 4.1.) One dimensional Voellmy-Salm model

The slide model is a generalization of the quasi-one-dimensional dense-snow avalanche model that contains a Voellmy-fluid flow law with longitudinal active and passive straining. The dense-snow avalanche flow is a hydraulic-based and depth-average continuum model that divides avalanche flow resistance into a dry Coulomb-type friction and a viscous resistance which varies with the square of the flow velocity. The models numerically solve the mass (volume) and momentum balance equations:

$$\frac{\partial A}{\partial t} + \frac{\partial Q}{\partial x} = 0 \quad (4.1)$$

$$\frac{\partial Q}{\partial t} + \frac{\partial}{\partial x} \left[ \alpha \frac{Q^2}{A} \right] + \lambda g A \left[ \frac{\partial h}{\partial x} \right] \cos \varphi = g A (S_o - S_f) \quad (4.2)$$

where  $g$  is the acceleration due to gravity,  $h(x,t)$  is the avalanche flow height,  $S_0$  and  $S_f$  are the acceleration and frictional slope, respectively,  $\lambda$  is the active/passive pressure coefficient and the  $\alpha$  is the velocity profile factor. The equations are based on several assumptions: flowing mass is a fluid continuum of mean constant density; the flow width,  $w(x)$  is known; a clearly defined top flow surface exists; the flow height,  $h(x,t)$  is the average flow height across the section; the vertical pressure distribution is hydrostatic and centripetal pressures which modify the hydrostatic pressure distribution are not accounted for; and flow velocity and depth are unsteady and non uniform.

The parameter  $\alpha(x,t)$  is the velocity profile factor. For a rectangular velocity profile,  $\alpha(x,t) = 1$ . The  $S_0$ , acceleration slope, is given by:

$$S_0 = \sin \varphi \quad (4.3)$$

where  $\varphi(x)$  is the inclination of the bed slope from the horizontal. The friction slope,  $S_f$ , is found by depth-averaging the shear stress gradient:

$$\rho g S_f = \frac{1}{h} \int_0^h \frac{\partial \tau_{zx}}{\partial z} dz = \frac{1}{h} [\tau_{zx}(h) - \tau_{zx}(0)] = -\frac{1}{h} \tau_{zx}(0) \quad (4.4)$$

It is assumed that no shearing deformation  $\gamma$  occurs in the avalanche body and at the top surface.

$$\gamma = \tau_{zx}(Z) = 0 \quad \text{for } 0 < z \leq h \quad (4.5)$$

The avalanche moves as a plug with a velocity that is constant over the depth of the flow,  $h$ . No fluidized shear layer exists since shear deformations are concentrated at the base of the avalanche; the shear layer is considered small compared to the avalanche flow height.

The basal shear resistance consists of a dry Coulomb-like friction and a Chezy-like resistance:

$$\tau_{zx}(0) = \mu \sigma_z + \frac{\rho g}{\xi} U^2 \quad (4.6)$$

The stress  $\sigma_z$  is the overburden pressure at  $z = 0$  and is dependent on the flow height:

$$\sigma_z = \rho g h (\cos \sigma) \quad (4.7)$$

A hydrostatic pressure distribution is assumed.  $U$  is the plug flow velocity. The parameters  $\mu$  and  $\xi$  are constants whose magnitudes depend, respectively, on material properties and the roughness of the flow surface.

The friction slope for a Voellmy fluid is:

$$S_f = \mu \cos \varphi + \frac{U^2}{\xi h} \quad (4.8)$$

The stress in the longitudinal direction is proportional to the hydrostatic pressure and is:

$$\sigma_z = \lambda \sigma_z \quad (4.9)$$

where  $\lambda$  is the so-called active/passive pressure coefficient. The difference between active (extension) and passive (compression) cases are based on the sign of the velocity gradient (strain rate) in the longitudinal direction,  $\partial U / \partial x$ ,

$$\lambda = \lambda_a \text{ for } \partial U / \partial x > 0 \quad (4.10)$$

$$\lambda = \lambda_p \text{ for } \partial U / \partial x \leq 0 \quad (4.11)$$

This allows different amounts of internal flow friction to be introduced depending on whether the plug is longitudinally pulled apart or compressed. Rankine's theory is applied to define the active/passive pressure coefficients:

$$\left. \begin{array}{l} \lambda_a \\ \lambda_p \end{array} \right\} = \tan^2 \left( 45^\circ \pm \frac{\phi}{2} \right) \quad (4.12)$$

where  $\phi$  is the internal friction angle, closely related to the angle of repose.

## 4.2) Two dimensional Voellmy-Salm model

The flow is treated as an unsteady flow on a two dimensional manifold (the mountain) with the flow velocity given by a two-dimensional vector field  $\vec{u} = (u, v)$  and the flow height  $h$  of the slide measured perpendicular to the mountain profile. The model considers only dense flowing slide; that is, heavy dense flows of constant density. The governing differential equations of mass and momentum conservation are:

$$\frac{\partial h}{\partial t} + \nabla \cdot (h \vec{u}) = 0 \quad (4.13)$$

and

$$\frac{\partial h \vec{u}}{\partial t} + \nabla \cdot (h \vec{u} \otimes \vec{u}) = \vec{f} - \frac{1}{2} \nabla \cdot \lambda h^2 \quad (4.14)$$

The vector  $\vec{f}$  defines the difference between the gravitational acceleration and friction. The parameter  $\lambda$  defines the active-passive flow pressure due to longitudinal straining of the flow body. In principle, the governing equations are similar to the shallow water equations, with the exception of the active/passive pressure term. By defining a vector of conservative variables  $\vec{U} = (h, h\vec{u})^T$ , the system of equations (4.13) and (4.14) can be concisely written

$$\frac{\partial \vec{U}}{\partial t} + \frac{\partial \vec{F}_1}{\partial x_1} + \frac{\partial \vec{F}_2}{\partial x_2} = \vec{G} \quad (4.15)$$

where  $x_1$  and  $x_2$  define the coordinate system of the manifold. The vectors

$$\vec{F}_1 \text{ and } \vec{F}_2 \text{ are } \vec{F}_1 = \begin{pmatrix} hu \\ hu^2 + \frac{1}{2} \lambda h^2 \\ huv \end{pmatrix} \quad (4.16)$$

and

$$\vec{F}_2 = \begin{pmatrix} hu \\ huv \\ hv^2 + \frac{1}{2} \lambda h^2 \end{pmatrix} \quad (4.17)$$

The vector  $\vec{G} = (0, f_1, f_2)^T$  contains the difference between the gravitational driving force and the friction in both coordinate directions. Typically,  $f$  consists of a dry Coulomb friction (dependent on the flow height  $h$ ) and an additional contribution proportional to the velocity squared.

$$f_1 = g_1 - f n_u \text{ and } f_2 = g_2 - f n_v, \text{ where } f = \mu g_3 + \frac{g_3 (u^2 + v^2)}{\xi h} \quad (4.18)$$

$g_1$ ,  $g_2$  and  $g_3$  are the components of the gravitational acceleration in the coordinate directions.

The friction parameters  $\mu$  and  $\xi$  define the amount of dry Coulomb friction and the velocity-dependent contribution. The friction parameters  $\mu$  and  $\xi$  are thought to depend on the slide volume.

Except for the right-hand-side vector  $\vec{G}$ , these model equations are similar to the Euler equations for a two-dimensional isentropic gas, or the two-dimensional shallow water equations.

### 4.3) Voellmy Salm and Frictional with a Lagrangian solution

The 2-dimensional set of governing equations are

$$\frac{\partial h}{\partial t} + h \frac{\partial u_x}{\partial x} + \frac{\partial u_y}{\partial y} = \frac{\partial b}{\partial t}, \quad (4.19)$$

$$\rho h \frac{\partial u_x}{\partial t} = \rho h g_x + k_x \sigma_z \left( \frac{\partial h}{\partial x} \right) + k_{yx} \sigma_z \left( -\frac{\partial h}{\partial y} \right) + \tau_{zx} - \rho u_x \frac{\partial b}{\partial t}, \quad (4.20)$$

$$\rho h \frac{\partial u_y}{\partial t} = \rho h g_y + k_y \sigma_z \left( \frac{\partial h}{\partial y} \right) + k_{xy} \sigma_z \left( -\frac{\partial h}{\partial x} \right) + \tau_{zy} - \rho u_y \frac{\partial b}{\partial t}, \quad (4.21)$$

where

- h is the flow height,
- $u_x$  velocity component in x-direction,
- $u_y$  velocity component in y-direction,
- g gravitational acceleration,
- $k_x, k_y, k_{xy}, k_{yx}$ , tangential stress coefficients, dependent on the tangential strain state,

$$\sigma_z = \rho h \left( g \cos \varphi + \frac{\bar{u}^2}{r} \right) \text{ is the normal stress } r \text{ the radius of the track and } \bar{u} \text{ the depth-averaged speed,}$$

At the moment there are two rheological can be implemented for the shear stresses  $\tau_{zx}, \tau_{zy}$ :

(i) Coulomb friction type

$$\tau_{zi} = -\frac{u_i}{|u|} \sigma_z \tan \phi_b, \text{ (}\phi_b \text{ is the bed friction angle)}$$

(ii) Voellmy fluid type

$$\tau_{zi} = - \left( \sigma_z f + \frac{\rho g u_i^{-2}}{\xi} \right), f(\tan \phi_b) \text{ and } \xi \text{ are friction parameters.}$$

#### 4.4) Understanding the Input Parameters in the Frictional -Voellmy Salm model

The friction parameters consists of a term dependent on the angle of the slope (called Coulomb friction angle,  $\mu$ ) and a term dependent on the square of the (turbulent) velocity obtained in imitation of the turbulent friction in fluid mechanics. This parameters are usually are taken as constant during the avalanche.

The parameters  $\mu$  and  $\xi$  are usually calibrated by fitting observed run-outs with the model. For turbulence coefficient,  $\xi$ , values between 1000 and 1800  $\text{m/s}^2$  with 1400  $\text{m/s}^2$  as an average, should be used for movements that move over deep, dense material, for example in old deposits. Values of 400-800  $\text{m/s}^2$  would be applicable for movements that flow over rough terrain covered with boulders and trees.  $\xi$  depends on track shape (laterally confined or unconfined) and bed roughness,  $\mu$  depends on avalanche volume and type (wet or dry).

It seems difficult to measure  $\xi$  directly from observed natural avalanches. Clear determinations are impeded by the changes of the flow regimes, first, in the upper part after fracture and at the beginning of run out. In both cases, the governing factor for the development of speed is only  $\mu$ .

For the  $\mu$  parameter, Voellmy proposed an increase with density in the form  $\rho/2000$  ( $\rho$  in  $\text{kg m}^{-3}$ ) (Voellmy, 1955). From observations it is assumed a decrease with speed of  $5/u$  ( $u$  in  $\text{m/s}$ ). From data collected, one can conclude that  $\mu$  decreases proportional with  $-1/3$  power of the volume (if run out distance is roughly inverse proportional to  $\mu$ ).

These frictional parameters have several properties:

- $\mu$  must be less than the starting zone slope, otherwise the movement cannot get started
- $\mu$  cannot be zero; otherwise the velocity could not decay to zero. Unless the path profile turns horizontal and if it does velocity decays in an infinite time  $\left(\frac{1}{t}\right)^{0.333}$ , which cannot represent the way in which a movement comes to a sudden stop.

- In the “turbulent” expression,  $\xi$  is positive. Otherwise friction would be cumulative with the force of gravity, speeding up the movement.

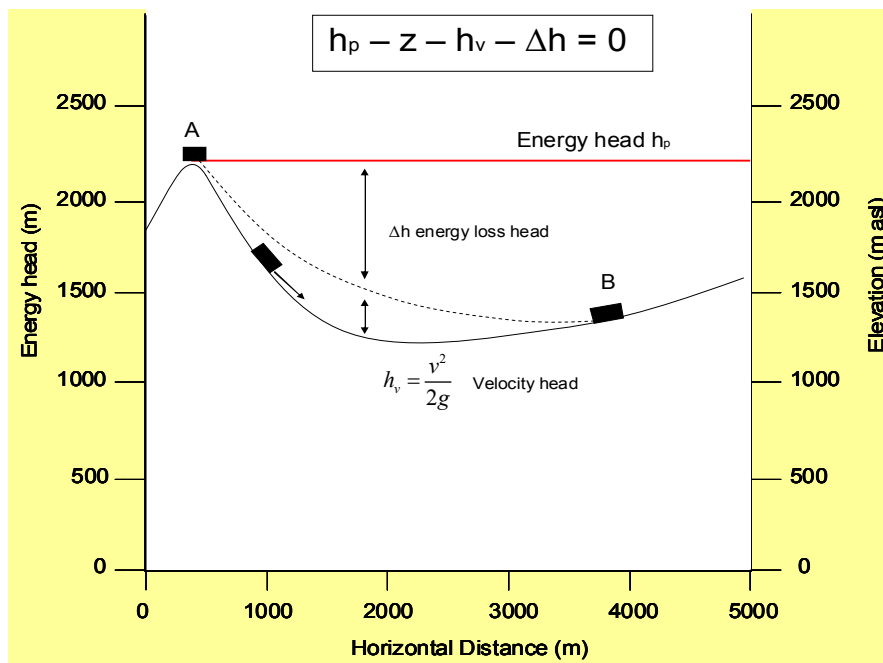
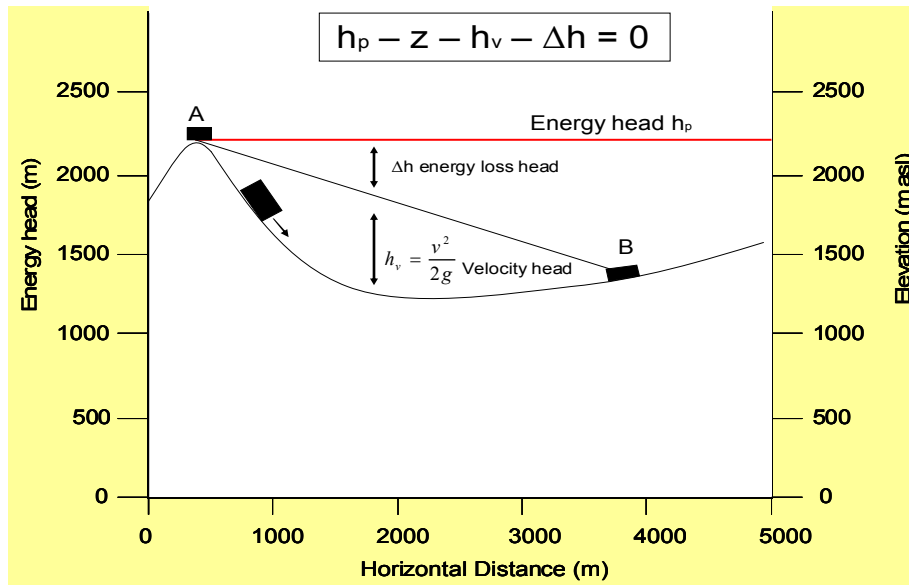
The parameter  $\lambda$  accounts for the efficiency of transfer of kinetic energy (particle speed) to potential energy (flow height). Salm considered avalanching snow to be a cohesionless material with internal friction, characterized by a friction angle  $\phi$ . This showed that surface wave propagation in flowing avalanches is impossible, so that the two modes in hydraulics “streaming” and “shooting” cannot exist. An important consequence of internal friction, are longitudinal “active” and “passive” stresses in the avalanche body. These stresses are assumed to be similar as in soil mechanics. The resultant critical force is  $R = \lambda \rho g D^2/2$ , with  $\lambda = \tan(45 \pm \phi/2)$ , where  $\rho$  density,  $g$  acceleration due to gravity and  $D$  flow depth. The positive sign in the expression for  $\lambda$  means passive, and the negative sign mean active state. If stresses are less than critical, the body is rigid and cannot deform. When velocity gradients however reach the critical value, deformation takes place. With increasing speed an elongation (active state), and with decreasing speed a compression (passive state) occurs. This is the consequence of the assumption of a rigid, perfectly plastic material. This procedure to calculate the internal deformation of avalanches is especially important for the dimensioning of deflecting and catching dams (Salm, 1993). Physically, it represents the internal energy dissipation during impact where yielding can safely be assumed.

#### 4.4.1) Linear model and non linear models and the need of a turbulent term $\xi$

The reason for the inadequacy of linear models is that they do not reproduce the non-linearity of the avalanche movement along the path profile, which itself is dependent on the specific rheology of each avalanche. In the VS model, the avalanche is considered as a solid block of mass sliding on a slope, with a friction applying an opposite force, dependant on the local slope and/or velocity.

The main differences between linear and nonlinear models can be seen in the deposits and in the velocities. . This can be explained with the help of the energy line as shown in the figure 3. For a frictional linear block moving from point A to B, the energy line is straight and inclined at the bulk friction angle,  $\phi_b$ . The velocity,  $v$ , of the block at any point in the path can be calculated from the energy head,  $v^2/2g$ , which equals the vertical distance between the energy line and the path. Prediction of lower velocities is possible only if the model includes a velocity dependent component such as a turbulent one,  $\xi$ , yielding the dashed, curved line in the diagram.





where  $h_p$  = energy head,  $z$  = elevation,  $h_v$  = velocity head,  $\Delta h$  = energy loss head

**Figure 3.** Energy distribution. The double headed arrows indicate the magnitude of velocity head,  $v^2/2g$  and the energy loss head,  $\Delta h$ . The full line represents energy head of the frictional model (top) while the dashed line corresponds to the Voellmy model which includes a turbulent coefficient,  $\xi$  (bottom).

#### 4.5) Quadratic model

The quadratic model is an Eulerian two-dimensional finite difference model conceived for routing non-Newtonian floods. It is based on a simple volume conservation model. The volume is moved around on a series of tiles to simulate overland flow (2D flow), or through line segments for channel routing (1D flow). Both topography and resistance to flow control flood wave progression over the flow domain. Flow in two dimensions is accomplished through a numerical integration of the equations of motion and the conservation of fluid volume.

The governing equations -originally presented by O'Brien - are the continuity equation

$$\frac{\partial h}{\partial t} + \frac{\partial h V_x}{\partial x} + \frac{\partial h V_y}{\partial y} = i \quad (4.22)$$

and the two-dimensional equations of motion

$$S_{fx} = S_{ox} - \frac{\partial h}{\partial x} - \frac{V_x}{g} \frac{\partial V_x}{\partial x} - \frac{V_y}{g} \frac{\partial V_x}{\partial y} - \frac{I}{g} \frac{\partial V_x}{\partial t} \quad (4.23)$$

$$S_{fy} = S_{oy} - \frac{\partial h}{\partial y} - \frac{V_y}{g} \frac{\partial V_y}{\partial y} - \frac{V_x}{g} \frac{\partial V_y}{\partial x} - \frac{I}{g} \frac{\partial V_y}{\partial t} \quad (4.24)$$

in which  $h$  is the flow depth and  $V_x$  and  $V_y$  are the depth-averaged velocity components along the horizontal x- and y-coordinates. The excess rainfall intensity ( $i$ ) may be nonzero on the flow surface. The friction slope components  $S_{fx}$  and  $S_{fy}$  are written as function of bed slope  $S_{ox}$  and  $S_{oy}$ , pressure gradient and convective and local acceleration terms.

The depth-integrated rheology is expressed (after dividing the shear stresses by the hydrostatic pressure at the bottom of the flow  $\gamma_m h$ ) as:

$$S_f = \frac{\tau_y}{\gamma_m h} + \frac{K \eta V}{8 \gamma_m h^2} + \frac{n_{td}^2 V^2}{h^{4/3}} \quad (4.25)$$

where  $S_f$  is the friction slope (equal to the shear stress divided by  $\gamma_m h$ );  $V$  is the depth-averaged velocity;  $\tau_y$  and  $\eta$  are the yield stress and viscosity of the fluid, respectively, which are both a function of the sediment concentration by volume;  $\gamma_m$  is the specific weight of the fluid matrix;  $K$  is a dimensionless resistance parameter that equals 24 for laminar flow in smooth, wide, rectangular channels, but increases with roughness and irregular cross section geometry; and  $n_{td}$  is an empirically modified Manning  $n$  value that takes into account the turbulent and dispersive components of flow resistance (the calculation of  $n_{td}$  is hardwired in the model).

The yield stress, the viscosity, and the empirically modified Manning  $n$  value are calculated as follows:

$$\tau_y = \alpha_1 e^{\beta_1 C_v} \quad (4.26)$$

$$\eta = \alpha_2 e^{\beta_2 C_v} \quad (4.27)$$

$$n_{td} = n_t b e^{m C_v} \quad (4.28)$$

where  $\alpha_1$ ,  $\beta_1$ ,  $\alpha_2$ , and  $\beta_2$  are empirical constants,  $C_v$  is the fine sediment concentration (silt- and clay-size particles) by volume of the fluid matrix,  $n_t$  is the turbulent  $n$ -value,  $b$  is a coefficient (0.0538) and  $m$  is an exponent (6.0896). The latter ( $b$  and  $m$ ) are fixed in the model, and cannot be modified.

## 5) Monte Carlo Analysis in a Quantitative Risk Assessment

Monte Carlo analysis is a method that uses statistical sampling techniques to derive the probabilities of possible solutions for mathematical equations or models. One use of Monte Carlo is to evaluate the probability of particular outcomes from risk assessment modeling. Monte Carlo analysis can be implemented as a tool to evaluate the uncertainty and the variability associated with natural hazards.

Monte Carlo analysis was initially developed in the 1940's and popularized by physics researchers Stanislaw Ulam, Enrico Fermi, John von Neumann, and Nicholas Metropolis. The name is a reference to the Monte Carlo Casino in Monaco. The use of randomness and the repetitive nature of the process are analogous to the activities conducted at a casino. Perhaps the most famous early use was by Enrico Fermi in 1930, when he used a random method to calculate the properties of the newly-discovered neutron. Monte Carlo methods were central to the simulations required for the Manhattan Project, though were severely limited by the computational tools at the time. Therefore, it was only after electronic computers were first built (from 1945 on) that Monte Carlo methods began to be studied in depth. In the 1950s they were used at Los Alamos for early work relating to the development of the hydrogen bomb, and became popularized in the fields of physics, physical chemistry, and operations research.

The Monte Carlo form of simulation "inverts" the typical mode of simulation, treating deterministic problems by first finding a probabilistic analog. Previous methods of simulation and statistical sampling generally did the opposite: using simulation to test a previously understood deterministic problem. As such, it is a tool that can be used for conducting probabilistic risk assessments. A probabilistic risk assessment is an assessment that estimates the probability or likelihood that particular risk values would

result from exposure to a hazard. When single values are used to describe risks in a Quantitative Risk Assessment (QRA), it is known as a deterministic risk analysis. In a deterministic risk analysis, it is implied that the determined risk values adequately represent the risk to the elements at risk and little or no information is provided about the probability that a particular value will result from the exposure to the hazard. Monte Carlo analysis is used to determine the probability of occurrence for the point estimates of a deterministic risk assessment and, in this way, deal with the uncertainty associated with these assessments.

Monte Carlo simulation considers random sampling of probability distribution functions as model inputs to produce hundreds or thousands of possible outcomes instead of a few discrete scenarios. The results provide probabilities of different outcomes occurring.

### **5.1) Probability density functions, uncertainty and variability**

One of the reasons to use a Monte Carlo analysis would be to examine the effect of uncertainty and natural variability on the estimate of risk. Uncertainty could be the result of measurement error, sampling error, model uncertainty (uncertainty due to simplification of real-world processes, incorrect model structure, misuse of models, and use of inappropriate assumptions), descriptive errors, aggregation errors, and errors in professional judgment. Since uncertainty refers to things that are unknown or unsure, the collection of additional site-specific information can reduce the degree of uncertainty.

Variability, on the other hand, refers to the differences in measurements or responses that are due to the true heterogeneity or diversity in a population or exposure parameter. Variability, usually measured as standard deviation or variance, represents natural random processes. Variability cannot be reduced through additional measurements or studies, although the uncertainty of variability can be improved.

The variability for a parameter can be represented as a probability density function (PDF), alternatively referred to in the literature as a probability function, frequency function, or frequency distribution. For a continuous variable (a variable that can assume any value within some defined range) the probability density function expresses the likelihood that the value for a random sample will fall within a particular very small interval.

Probability density functions are used as the basis of a Monte Carlo analysis and the proper selection of PDF's is essential for a good analysis. Probability density functions can take on a variety of shapes. Examples of some PDF's include normal, lognormal, exponential, uniform, Poisson, and binomial distributions and each of these has distinctive characteristics. In addition, custom probability functions that do not fit any of the theoretical distributions can be derived for a particular parameter by using the frequencies at which particular values for the parameter are observed. The PDF selected for each input parameter in a model will be used to identify the likelihood that particular

input values will occur when a Monte Carlo analysis is applied. The shape of PDFs can greatly affect the outcome of a Monte Carlo analysis and must, therefore, be selected with care.

## 5.2) Application of a Monte Carlo analysis

In a deterministic model, a single value for each of the model's input parameters is used to calculate a single output parameter. To conduct probabilistic modeling using Monte Carlo analysis each of the input parameters is assigned a distribution. The output from the model is calculated many times, randomly selecting a new value from the probability distributions for each of the input parameters each time. The outputs from each run of the model are saved and a probability distribution for the output values is generated. This allows the probability of the occurrence of any particular value or range of values for the output to be calculated. Figure 4 presents a representation of how Monte Carlo analysis is conducted.

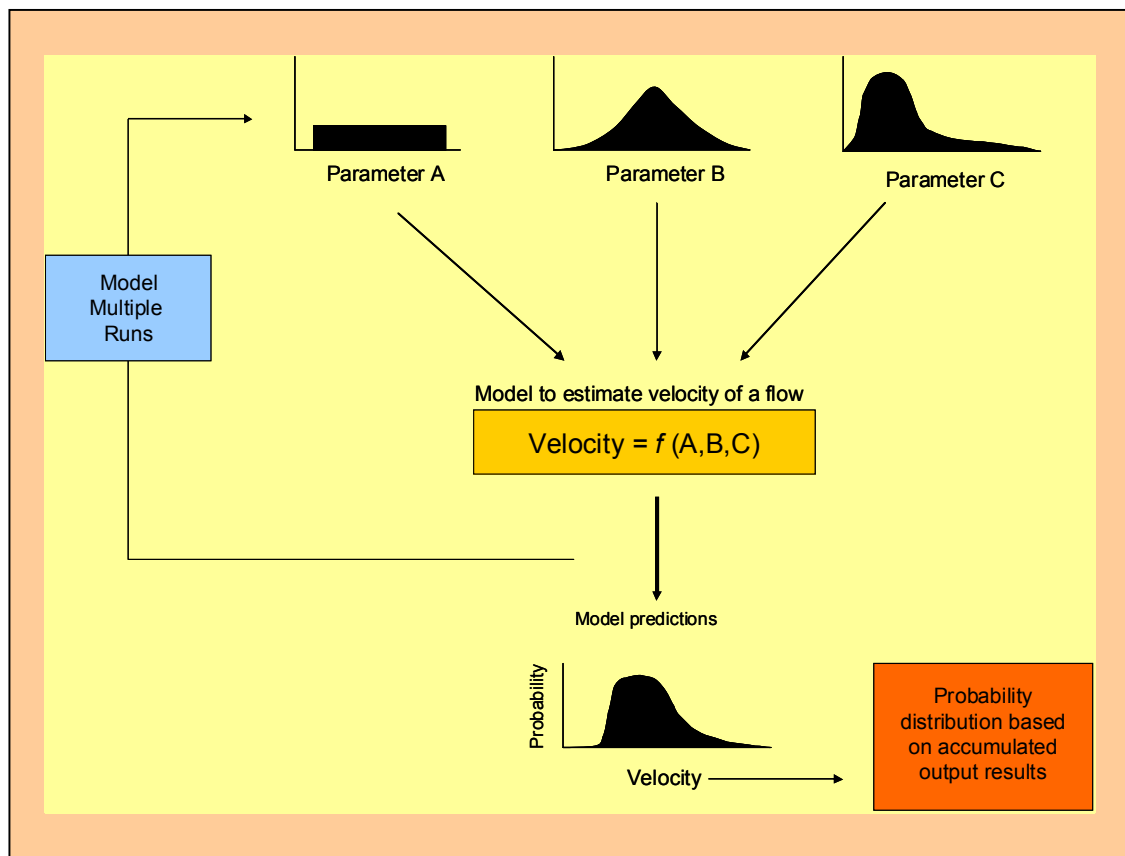


**Figure 4.** Representation of a Monte Carlo analysis for a run out model

### **5.2.1) Defining the statistical distributions of input parameters**

Defining the statistical distributions (PDFs) that will be used for the model's input parameters is probably the most difficult aspect of a Monte Carlo analysis. It is tempting to make assumptions about the distribution of particular input parameters when insufficient information is available to reliably determine what the actual distribution is. However the shape of the probability distribution can greatly affect the outcome of the Monte Carlo analysis and it is extremely important that an appropriate distribution be selected.

It should be noted that Monte Carlo analysis does not require that PDF's be defined for all input parameters. In multiple-parameter models where there is no basis for assigning a PDF to particular parameters, it is acceptable to keep a fixed value for those parameters while assigning PDF's to parameters where sufficient information is available.

### **5.2.2) Repetition of the model**

Once the PDF's for the input parameters have been defined, a computerized routine is used to repeatedly run the model with input parameter values selected according to the probabilities identified in the PDF's. Typically, the model is run hundreds or thousands of times.

### **5.2.3) Outputs of a Monte Carlo Analysis**

After each run of the model has been completed, the output value is saved. After all the simulations have been completed, the frequency with which particular output values were obtained is analyzed. The resulting set of output values can be evaluated to determine descriptive statistics such as the mean, range, standard deviation, etc. In addition, it is possible to evaluate the probability that the outcome will exceed a particular value or will fall within a certain range of values.

Another potential use of Monte Carlo analysis is for examining the sensitivity of a model to changes in specific parameters about which there is a high degree of uncertainty. To do this, the values of all input parameters in the model, except one, are held as fixed values. By allowing the single remaining parameter to vary in a Monte Carlo analysis, the effect of different values of that parameter on the outcome of the model can be examined.

## **6) A Monte Carlo approach for run out models**

## 6.1) Monte Carlo approach for frictional and Voellmy model

The use of run out models in a quantitative risk assessment can become problematic as these models are not really physically-based models. For instance, they do not include all the phenomena occurring in the mass movement, and the rheological behavior of the flow is not known. So, it is not easy to predetermine the extreme events extensions. For this reason a Monte Carlo analysis can be performed to be able to deal with these uncertainties. The procedure is to fit the parameters used in a dynamic numerical model, (friction coefficients and the volume of the flow involved) to the field data. Then, using the obtained parameters as random variables, appropriate statistical distributions will be adjusted. The last steps involve simulating a large number of (fictitious) flows using the Monte Carlo approach. In this way, the cumulative distribution function of the run-out distance can be computed over a much broader range than initially with the historic data. This approach will be used in different locations and different types of mass movements (snow and debris flows) through complete case studies, using two different models for comparison (Coulomb frictional and Voellmy-Salm).

In a dynamic model, the flow features are deduced from solving the equations of motion (mass and momentum equations). Deterministic models (sliding-block and depth-averaged models) introduce a friction law, reflecting the interaction between the flow and the path. In most models, the friction law includes two empirical frictional parameters, which have been fitted from field observations (Voellmy-Salm model). Though it aims primarily at providing a physical picture of a motion, the deterministic approach involves too many assumptions to be considered as a true physical approach. Also, very little is known on the bulk rheological behavior and despite a number of attempts to find physical justifications for their expressions, the friction laws used so far remain empirical. This means that the parameters do not represent physical properties of the flow (like viscosity) but, reflect the influences of the flow, path profile, and model assumptions on the computations. This allows us to question the use of dynamics models to paths where no field data are available.

With a Monte Carlo technique it is possible to determine the dependency between the probability distribution of input and output variables for a given path. Where the flow will be used as a sliding block and a Coulomb-like model (one parameter model) and a Voellmy-like model (two parameter model) will be used as the mathematical operators for simulating the main features of the flow motion.

The basic idea is to assume that there is a relationship  $G$  between the run-out distance, velocity, pressures, depths and other field data. This means that it is needed to have distinctive types of field data. These will include the starting point elevation, the released volume and so on. These field data will be the input variables. It is expected that  $G$  also

depends on the topographical features of the path and on a set of structure parameters, reflecting the variability the flow motion.

If the input variables and/or the internal parameters are random, then the run-out outputs are also random variables. If it is possible to adjust the internal parameters for the computed run-out outputs to match the observed run-out event, then it is possible, by using Monte Carlo simulations, to create a large number of fictitious events coherent with the observations. If the run-out outputs sample is large enough, it will be possible to fit an empirical probability distribution and then accurately determine the quantile related to a low occurrence probability.

This can be divided into the next steps

A distribution function will be fitted to structure parameters (flow density, flow rheology) using data from various well documented torrents in the French and Italian Alps.

Second, random input parameter will be generated by using probability density functions. To avoid confusing results of simulations, the randomly generated inputs will be evaluated to avoid impossible parameter combinations.

Third, model runs will be performed using the randomly generated input values. The model will simulate the flow height, flow pressures and flow velocity.

Fourth, the spatial probability of occurrence is estimated considering all the model runs.

Finally the degree of hazard, expressed as a time probability will be obtained. A very large sample of runs will be obtained. We then deduce the empirical probability density function of the outputs. This function must approximately match the empirical distribution adjusted from the recorded events but, since it results from a much larger sample, it extends over a wider range of probabilities. This will allow to accurately compute the quantile associated with a low non-exceedance probability.

### **6.1.1 Frictional (Coulomb-like friction) model**

For the first step, we will chose the input and output variables: the starting zone volume and run-out outputs. By fitting the model, we will obtain the sample of friction parameters.

For the second step, we will fit the sample of starting volume zone values into a probability distribution. Then we will fit a distribution to the friction parameter

In the third step, we will create a large sample of staring zone volumes and friction values using a random number generation routine.

In the last step, we will use the samples to generate significant amount of fictitious flows. The run-out distance of each event will be stored. The simulated run-out should match well the field data.

### **6.1.2) Voellmy Model**

The Voellmy model involves two internal parameters (a frictional term  $\mu$  and a turbulent term  $\xi$ ). Since we have only want one output variable, the value of one of them must be kept constant for the inverse problem to be solved.

Determining the statistical distributions on both input parameters seems to be a difficult task since it is not possible to use a one-peak distribution fitted to the data. Maybe the simplest approximation involves taking the sum of the two probability distributions fitted on each group. In this way, we shall obtain the one-variable conditional distribution of each parameter but this is yet to be confirmed.

The third step is to randomly generate a sample of values for the release volume from its empirical probability distribution. In a similar way, generate values of the internal parameters from the different conditional distribution of  $\mu$  and  $\xi$ .

In the fourth step, the run-out outputs have to be computed by simulations and fitted into a probability density function.

## **6.2) Monte Carlo approach for Quadratic model**

In this model a discharge hydrograph is needed as an input. When used as a routing model, the discharge will be distributed in two dimensions according to the friction and viscous parameters selected. Usually, the friction and viscous parameters have been derived from experimental data and for this reason the discharge hydrograph plays an important role as an input parameter.

A Monte Carlo simulation approach will be adopted in which a stochastic model of rainfall will be used to generate a long artificial input series to the quadratic model; the required magnitude–frequency relationship can then be estimated from the derived artificial output series.

An artificial long series of continuous hourly rainfall will be generated. The main storms will be divided from hourly rainfalls to minute rainfalls. For each artificial storm it will be checked whether a debris flow can be triggered, by comparing the rainfall intensities of the artificial storm to the rainfall intensity threshold (already calculated for the area).

The storms that will generate debris flows will be identified. Discharge hydrographs will be computed by means of a rainfall-runoff analysis. The values of the frictional parameters of the quadratic model will be calibrated and as in the Frictional and Voellmy routine, the parameters will be approached with a Monte Carlo technique. Concentration discharge hydrographs will be calculated by means of concentration formulas taking into account the debris flow discharge, the concentration of the static bed, the solid concentration, the internal friction angle and the angle between the bed and the horizontal plane.

For each simulated debris flow, maximum values of flow velocity, water depth and total force per unit width will be collected in each node of the computational domain and non exceedance probability functions will be estimated for the three variables.

The Monte Carlo simulation technique will allow to include the uncertainties related to model parameters (density of solid fraction, yield stress, Manning roughness coefficient). and the variability will be reflected by their statistical distributions. Therefore, the choice of these distributions is of great importance, especially for the variables or the parameters that may reach large values ( $\xi$  in the Voellmy-like model) or come close to zero ( $\mu$  in the two models).

## 7) Field Test Sites

### 7.1) Barcelonnette Basin/Faucon, France

The Barcelonnette Basin (Figure 5), located in the South French Alps, has an elevation ranging from 1100 to 3000 m a.s.l, slope gradients range from 20° to 50°. The Basin is a geological window in two Eocene crystalline sheet thrusts (flyschs from the Autapie and the Parpaillon) that overlay the black marl (Figure 6). The thickness of the Jurassic black marls reaches 250-300 m, they present grey clayey schist facies and more calcareous black facies, very finely laminated. The black marls and the weathered flyschs are mostly covered by moraines and/or slope deposits. The land use is made of forests (60%), progressive abandon of agricultural lands and bare lands with intense gullying. The Barcelonnette Basin has a dry and mountainous Mediterranean climate with a strong inter-annual rainfall variability ( $733 \pm 412$  mm over the period 1928-2002), strong storm intensities (over 50 mm.h<sup>-1</sup>) and 130 days of freezing per year (Figure 7).

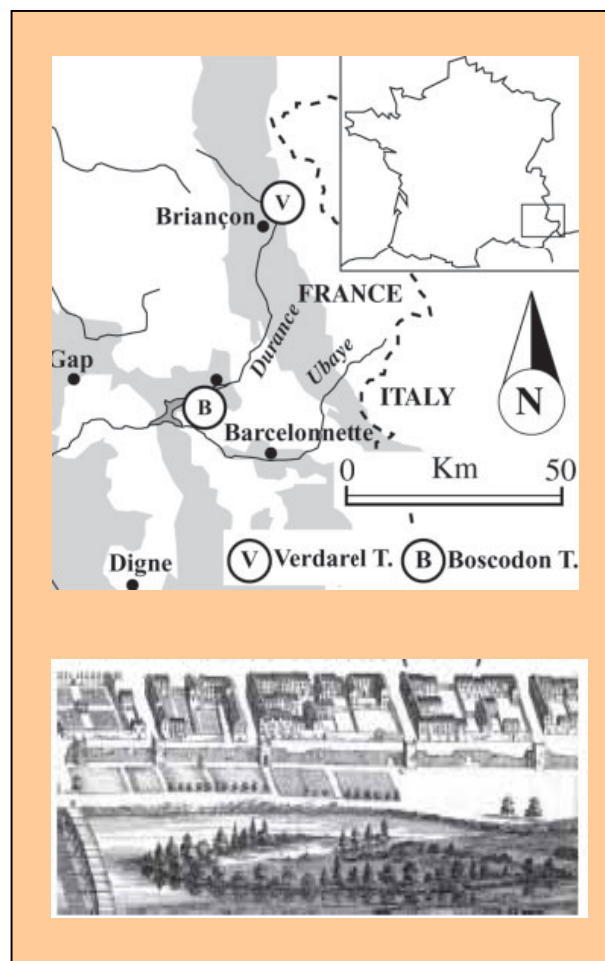


**Figure 5.** Location of the Barcelonnette basin

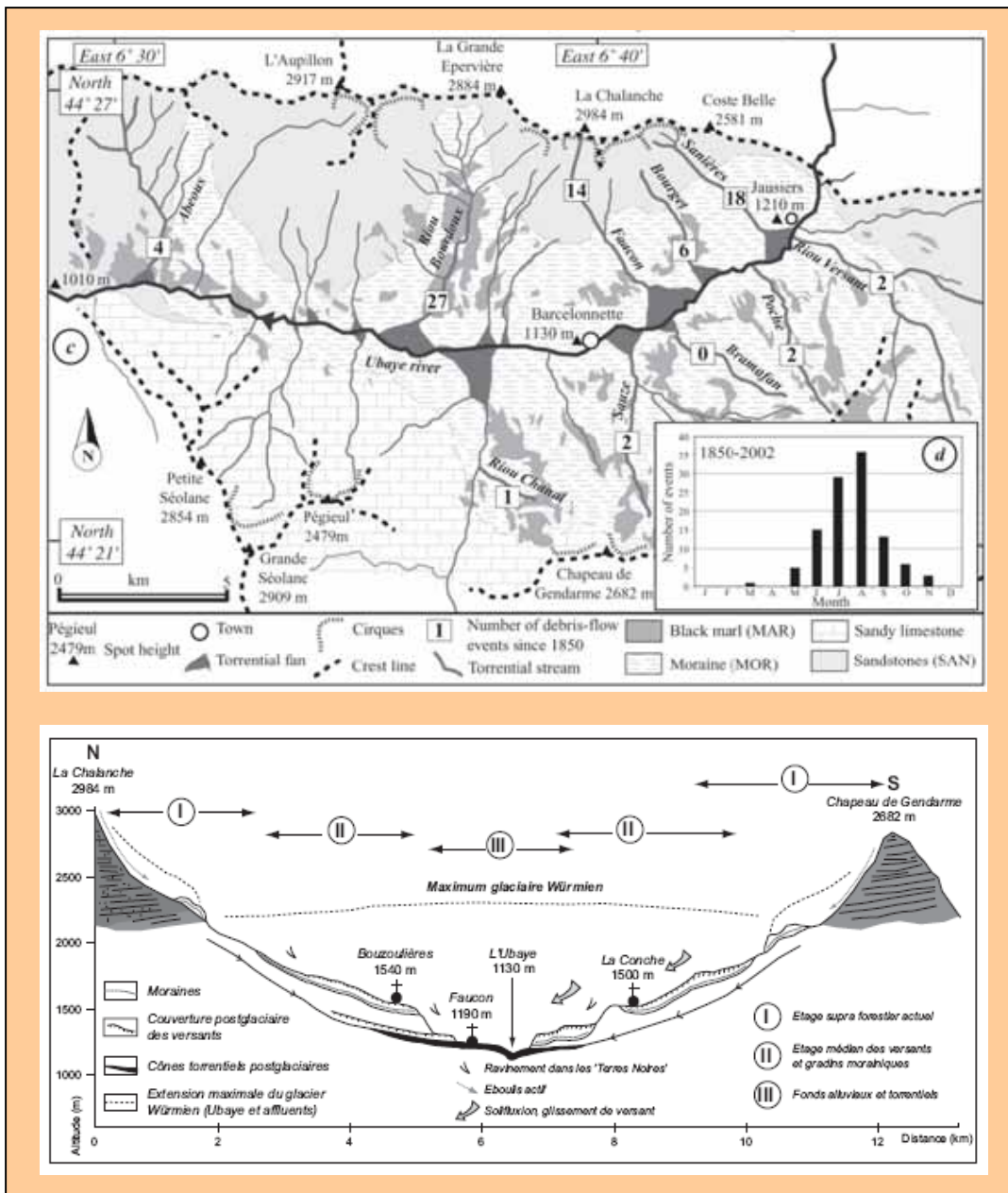


**Figure 6.** Barcelona basin and extent of the black marl (gray). Profile of the path of ten torrential stream, morphological sketch and monthly occurrences of events since 1850 (above). Profile of the Barcelona basin (below)

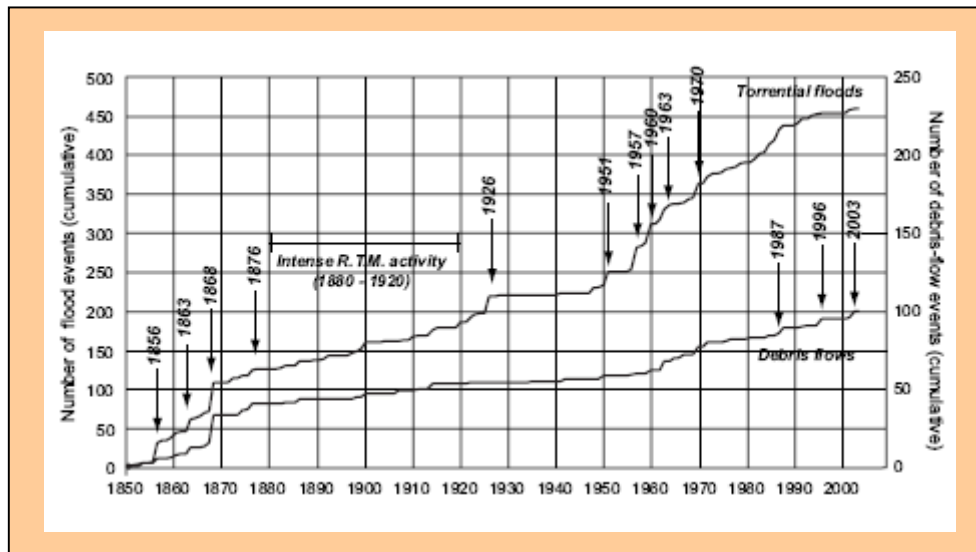


**Figure 7.** Flood and Debris flows events occurred in the Barcelonette basin since 1850.

### 7.1.1) Faucon description and events

The Faucon basin (44°25'N, 6°40'E) is a steep forested watershed with an area of approximately 10.5 km<sup>2</sup> which rises to 2984 m a.s.l. (Figure 8) Local slopes are steeper than 25°, reaching 80° at the highest elevations. The higher parts of the massif consist of two sheet thrusts of faulted sandstones and calcareous sandstones. Slopes below this consist of Callovo-Oxfordian black marls, mainly composed of fragile plates and flakes packed in a clayey matrix. Most slopes are covered by various Quaternary deposits: thick taluses of poorly sorted debris; morainic deposits; screes and landslide debris. These deposits have a sandy-silt matrix, may include boulders up to 1–2 m in size and are between 3 and 15 m thick.

The incised channel has an average slope of about 20°, ranging from 80° in the headwater basin to 4° on the alluvial fan, and is approximately 5500 m in length. Channel morphology is characterized by two main types of cross-section: a V-shaped profile with a steep channel, and a flat-floored cross-profile between steep slopes. The Faucon torrent has formed a 2 km<sup>2</sup> debris-fan that spreads across the Ubaye valley floor (Figure 8). It has a slope gradient ranging from 4 to 9°. The fan consists mostly of cohesionless and highly permeable debris (debris-flows strata and/or torrent deposits).

The climate type is continental with Mediterranean and mountainous influences, with strong rainfall differences during the year (733 ± 412 mm over the period 1928-2002) and strong storm intensities (over 50 mm.h<sup>-1</sup>). The Faucon stream has a classic torrential flow regime associating: (1) peak discharges in spring (snowmelt) and in autumn (high precipitation) and, (2) a high variability in summer according to the occurrence of storms.

Since 1850, 14 debris flows have occurred in the Faucon torrent. More than 70 check dams were built on the torrent since the 1890s to prevent flooding but only half of them are still efficient (Figure 9)(Remaître *et al.*, 2005).

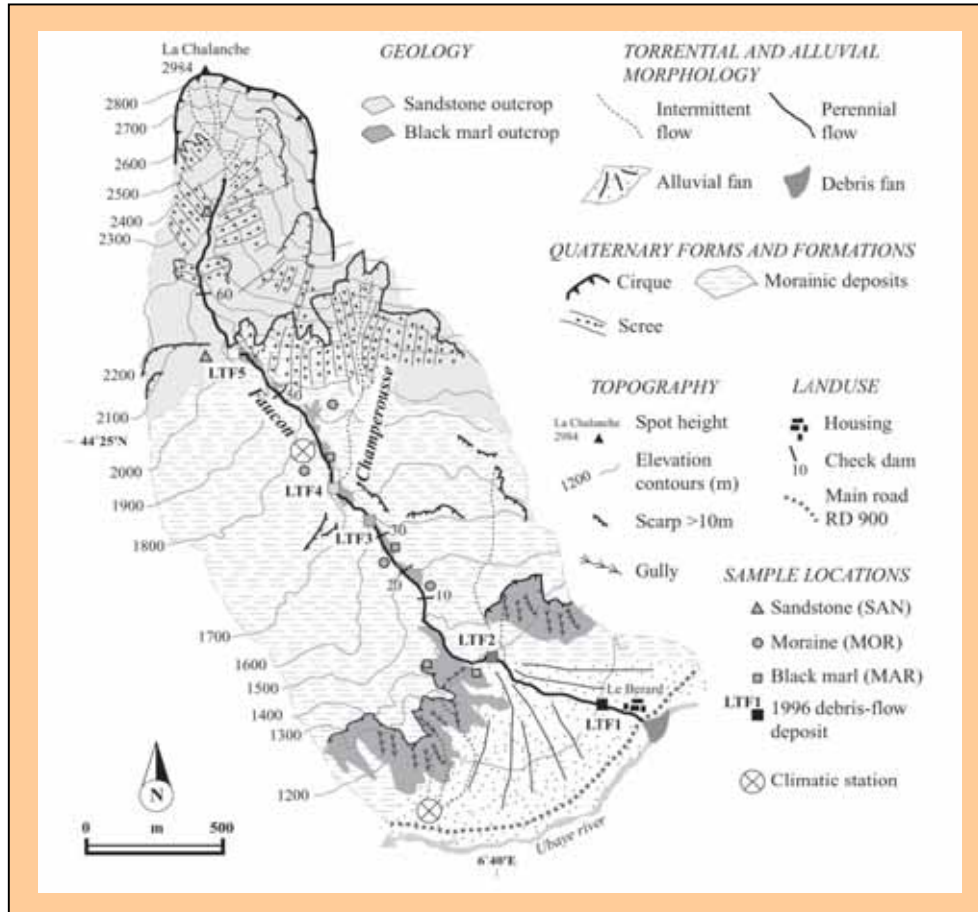


**Figure 8.** Morphological map of the Faucon watershed



**Figure 9.** Check dams built in the Faucon basin

- Debris Flow 19 august 1996 (Remaitre, 2005)

On 19 August 1996, a debris flow was triggered by an intense and local thunderstorm. According to eye-witnesses and the French Forest Office, the total duration of the event was about 2.5 hours. The debris flow caused moderate damage and the main road across the alluvial fan was cut for several hours.

The source area of the debris flow (above 2100 m a.s.l.) consisted of several shallow landslides of moderate size (<100 m<sup>3</sup>) on slopes ranging from 30° to 50°. In this section the channel width ranged from 5 to 8 m. The headwater basin has a rocky sandstone substrate, which has been exposed over several square meters by stripping of the surface gravel. This suggests removal of this loose, cohesionless material by sheet flow. The concentration of this loose unconsolidated material behind a natural dam and then the breaking of this dam caused the debris flow. A splatter of fine-grained liquid sediments was found up to 6 m high on trees along both sides of the debris-flow source area which allows an estimate of the height and volume of the breached dam (approximately 5000 m<sup>3</sup> of debris-flow material, (Remaitre *et al.*, 2002).

One thousand meters below the initiation point at the black marl outcrop, the flow path widened by 10 m. The total length of the transport zone is 3000 m with a slope gradient of about 25°. Several areas of erosion were observed, characterized by shallow weathered black marls and/or Quaternary deposits sliding over the bedrock. During passage of the flow, channel bed scour increased the volume of the debris flow, especially by incorporation of the material from the black marls outcrop (1900 to 1300 m a.s.l.). The scour depth of the surficial cover ranged between 0.5 and 2.0 m. Depending on the channel slope and shape, small lobate deposits (thickness ranging from 0.20 to 1.0 m) of debris-flow pulses could be observed. Lateral and channel-bed deposition occurred downstream between 1300 to 1750 m a.s.l., and formed discontinuous narrow levees rising 2–3 m above the surrounding slopes on both sides of the channel. A strong inverse grading has been observed. Lateral sorting of the debris deposit was poor to very poor, whilst vertical sorting was high. The size of the levees may exceed 100 m in length and 30 m in width. Mapping of the debris-flow deposits in the path allowed us to estimate the volume at approximately 11 000 m<sup>3</sup>.

Most of the debris flow spread over the old (pre-1996) alluvial fan and joined the Ubaye River. The 1996 debris-fan was about 100 m long and 250 m wide, with a thickness ranging from 1.5 to 3.0 m. Its volume was approximately 50 000 m<sup>3</sup>.

- Debris Flow 5 august 2003 (Remaitre,2005)

The debris flow has been triggered on two specific spots on the east flank of the Faucon catchment: the Trois Hommes area, and the upper part of the Champerousse torrent (a tributary of the Faucon stream). For both cases, the morphology of the source area corresponds to a strong incision in scree slopes.

In the Trois Hommes area (Figure 10), the depth of the incision is about 2 m; the debris flow track widened from 2m at the head scarp to 5 m at the confluence with the Faucon torrent, the 750 m farther downslope. Thus, the volume of the Trois Hommes debris flow ranged approximately from 4,000 to 5,000 m<sup>3</sup>. No evidence of temporary damming was observed at the confluence, suggesting that the Trois Hommes debris flow immediately flowed in the Faucon torrent main track.

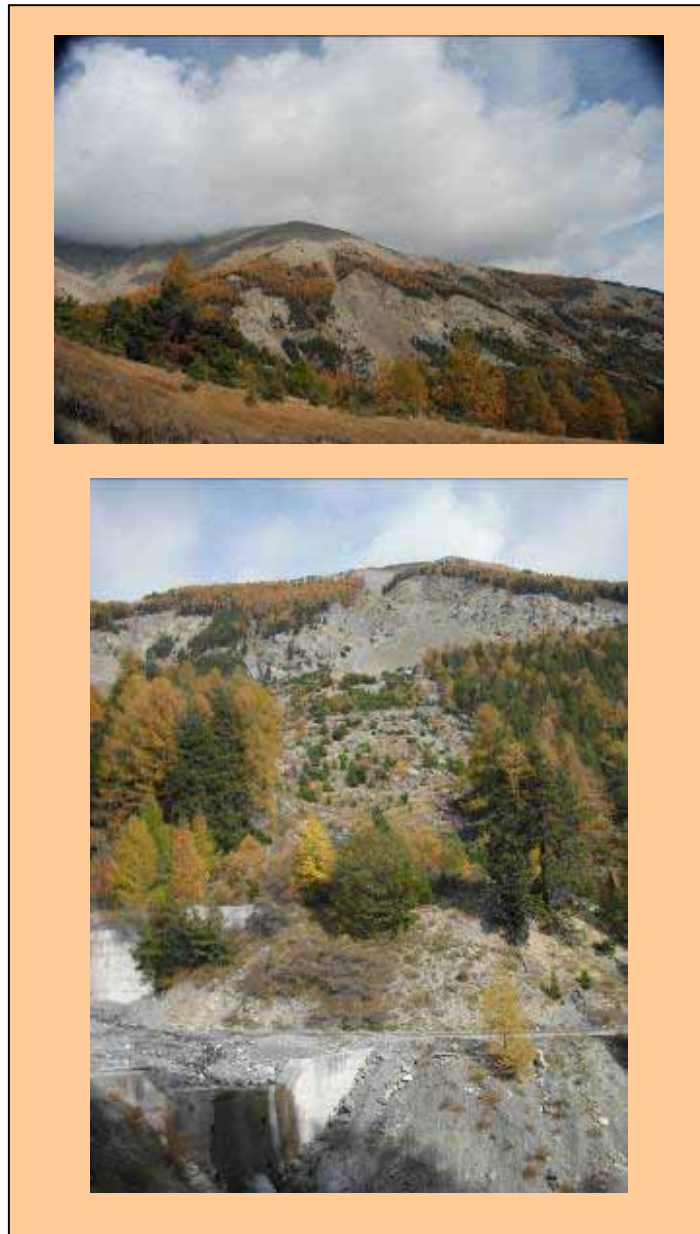


**Figure 10.** Different view of the Trois Hommes area

In the Champerousse torrent (Figure 11), the depth of the incision ranged from 2m in the upper part to 1 m in the lower part; the width of the debris path is about 3 m. The volume of the material in the source area ranged from 6,000 to 7,500 m<sup>3</sup>. Unlike the Trois Hommes event, all the material did not reach the Faucon torrent; in fact 3,000 m<sup>3</sup> has been trapped by the check dams, some morphological evidence shows that the Champerousse debris flow transformed into a hyperconcentrated flow.



**Figure 11.** View of the Champerousse torrent

The observations at the Trois Hommes slope and the Champerousse torrent indicate that the source volume ranges from 7,500 to 9,500 m<sup>3</sup>.

Field measurements and evidence of the residents indicate that the debris flow evolved into 5 surges, for a time interval ranging between 2 and 5 minutes. These debris flow surges filled progressively the channel. Eyewitnesses indicate that the debris flow height of the last surge reached 5 to 6 m. Most of the debris spread over the left bank, causing some substantial damages on five houses (Figure 12)



**Figure 12.** House affected by the 2003 Faucon debris flow.

According to the measured area and the depth of the deposits both in the channel and on the fan the total volume of the debris flow deposit was estimated to be  $45,000 \text{ m}^3$  on the debris fan and  $15,000 \text{ m}^3$  in the upper channel.

Channel scouring was responsible for the great difference of  $7,500\text{-}9,500 \text{ m}^3$  of the two source areas and the  $60,000 \text{ m}^3$  of the total volume of the debris flow solid material. The total length of the flow track is about  $3,500 \text{ m}$ , with a slope gradient of  $15^\circ$ . Several areas of scouring mainly took place in the 1996 debris flow deposits area. The channel scour rate amounts to  $15 \text{ m}^3 \cdot \text{m}^{-1}$ . Observations indicate that the scour rate depth ranges between  $0.5$  and  $4 \text{ m}$ .

The debris flow event started as a granular flow, bulked increased in fine elements by incorporating marly sediments along the flow track and transformed into a muddy debris flow. Such phenomenon has been observed during the 1996 event.

Relations between the 1996 and 2003 events seem to be very close. The volumes of the two events are quite similar.

## 7.2 Valtellina valley/Selvetta , Italy

Within Valtellina there is a consortium of 12 municipalities (Mountain Consortium of Communes of Valtellina di Tirano) The total study area is of about 300 km<sup>2</sup> with a population of about 30,000 inhabitants (Figure 13).

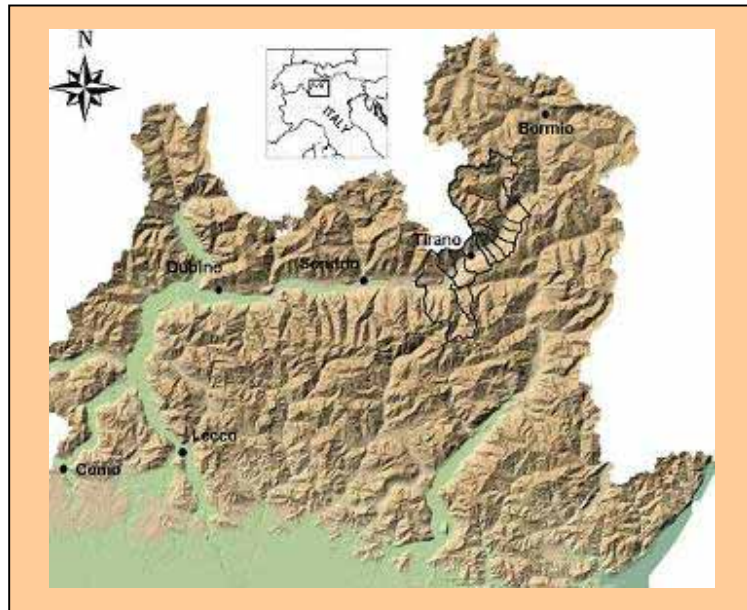


**Figure 13.** Location of the Valtellina Valley

Valtellina is an important Italian valley located in Central Italian Alps (Northern Italy, Sondrio Province). The valley stretches out in an E-W orientation from Dubino (where the valley joins the Como lake) to Teglio, where it takes a north-easterly turn for a few kilometers, then turns almost due north around Sondalo.

The valley is superimposed on a regional fault that sharply separates the properly-called Alps (Austroalpine, Penninic and Helvetic nappes) to the north from the Variscan basement of the Southern Alps to the south. The Periadriatic Fault, commonly known in Lombardy also as Insubric Line or Tonale Fault, has a mostly E-W trend in Lombardy, running on the northern slopes of Valtellina, some 500 m above the Adda River floodplain. Then, the tectonic line goes on towards NE, from Tonale pass to Merano and Mules, near Vipiteno, where it shows again an E-W trend running along Val Pusteria up to Klaghenfurt and beyond. The bedrock (the pre-Alpine metamorphic basement) is mainly composed of metamorphic (gneiss, micaschist, phyllite and quartzite) and intrusive rock units, with subordinate sedimentary rocks. Due to the proximity of this tectonic lineament, cataclastic and mylonitic zones are present in the bedrock (Figure 14).

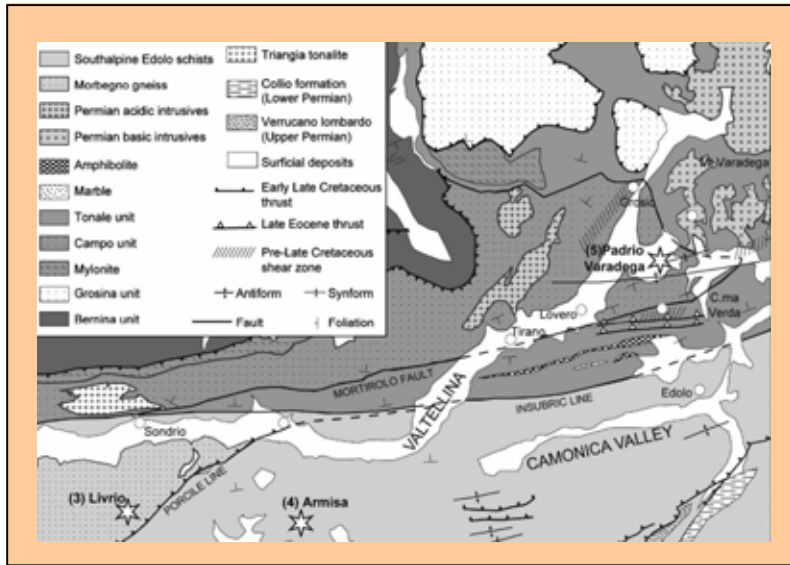


**Figure 14.** Geological map of the Valtellina valley

Valtellina represents the upper drainage basin of the Adda river, which flows in a flat alluvial plain up to 3 km wide. Alluvial fans at the outlet of tributary valleys can reach a considerable size, with a longitudinal length up to 3 km. The elevation of the valley bottom ranges from 200 m a.s.l., where the Adda river joins the Como lake, up to 400 m a.s.l. near Tirano (where the valley takes a north-easterly turn), up to 1,225 m a.s.l. at Bormio (where the valley ends). Valtellina has a U-shaped valley profile derived from Quaternary glacial activity. The lower part of the valley flanks are covered with glacial, fluvio-glacial, and colluvial deposits of variable thickness (Figure 15).

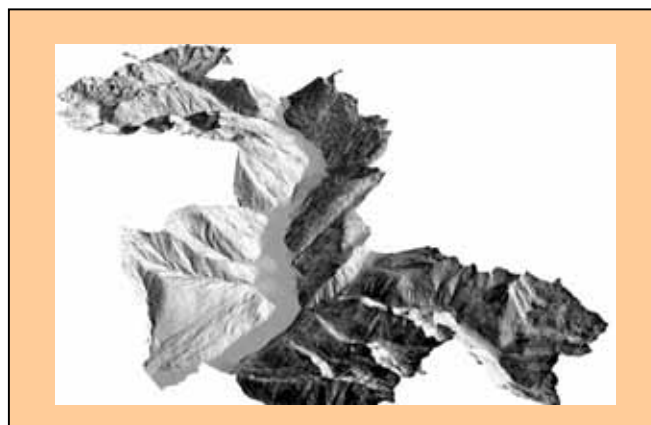


**Figure 15.** View of the Valtellina valley

Valtellina has a history of intense landsliding. Landslides are among the most significant natural damaging events; they are one of the primary causes of life injury and property damages, resulting in enormous casualties and huge economic losses in that mountainous region.

A large number of landsliding events affected Valtellina on 14 - 17 November 2000. A prolonged and intense rainfall event triggered 260 shallow landslides on an area of 270 km<sup>2</sup>, most of them occurring on terraced slopes. This area suffered other intense landsliding phenomena on 1983 and 1987. On May 1983 a severe meteorological event triggered more than 200 shallow landslides, with a failure density of 60 landslides per km<sup>2</sup>, causing 17 casualties in Tresenda. The July 1987 event claimed 12 lives and triggered several hundreds of soil slips.

During the period 12-28 November 2002, Lombardy's pre-Alpine belt suffered heavy and prolonged rainfalls, unlikely to be repeated in over 100 years. This precipitation was accompanied by temperatures well above the average for the season, and the freezing point was reached only above 2000 m. Many landslides occurred in that period: field surveys allowed to map a total of 260 landslides, 146 of which are shallow soil slips or slumps and the remaining are soil slip-debris flows affecting Quaternary covers. Soil slips and slumps are characterized by small size and thickness (up to 1.5m), with volumes up to few cubic meters. These phenomena removed portions of cultivated areas, caused the interruption of transportation corridors and disruptions in inhabited areas determining the temporary evacuation of people.

Landslides sometimes occurred in areas of runoff and sub-superficial flow convergence. In other cases they are associated to the reactivation of older soil slip-debris flows scars. The maximum landslide density of about 4.4 landslides per square kilometer has been observed near Dubino. This value of landslide density has been computed on wooded areas up to the lower limit for snow cover (1300 m a.s.l.) on November 2000. An average landslide density of 11.5 failures per square kilometer has been determined on terraced terrain. The maximum values have been observed at Bianzone (49.0 landslides/km<sup>2</sup>) near Tirano, and at Cino (26.8 landslides/km<sup>2</sup>) near Dubino.

The need of cultivable and well exposed areas determined the extensive anthropogenic terracing of a large part of the valley flanks (Figure 16). The average terrain gradient of the slopes is 42°. Vertical dry stone walls retain terraces with mean terrain gradient ranging between 15° and 25°. The renewed morphology determines also variations in the sub-surficial hydrology of the slopes. An artificial drainage network (named "valgelli") has been realized in order to regulate flowing water. These works locally vary in shape and arrangement. In some cases, paths are used both as passages within the different orders of terraces and as drainage structures.



**Figure 16.** View of the terraces built in the Valtellina valley flanks

Landslides are a quite recurrent phenomenon in some of these settings. They are prevalently represented by soil slips, soil slumps and soil slip-debris flows. They damage cultivations, settlements and pose hazard to the safety of people. Their considerable hazard potential is related to the abundance of susceptible areas, the high areal density and the high velocity of the movements. These shallow landslides can be triggered by rainstorms of high intensity and short duration or by prolonged rainfall of moderate intensity, and by snow melting.

The occurrence of landslides cannot be explained by taking into account only the stratigraphical aspects. In fact similar stratigraphical settings can be found over wide areas, but landslides took place only at specific sites. The hydrologic and hydrogeologic factors must be considered. Some months after the occurrence of landslides many source areas still showed water seeping along the horizons which acted as failure surfaces. Water convergence in hollows has been recognized as an important factor in governing water supply at landslide source areas, but other processes have been identified, some of which specific of terraced areas. The rising up of shallow groundwater tables was recognized as responsible for landslide triggering at few sites

About 75% of slope failures occurred on November 2000 took place on terraced areas, and are mostly represented by soil slips and slumps. The prevailing landslide typology observed in woodland is soil slip-debris flows, with instabilities affecting Quaternary deposits up to 4 m. The total number of soil-slip-debris flows, including those occurred in hollows and at old slide scars is similar. The number of soil slips and slumps is ten times greater in terraced areas than in woodland. Source areas of debris flows on terraced areas are characterized by a modal width of 8 m, but scars up to 20 m wide have been mapped. The thickness of Quaternary deposits at source areas range from 0.5m to 2.5 m. The profile of the failure surface at source areas varies from curvilinear or almost straight to undulated and it suggests a retrogressive distribution of activity.

Mean slope angle of the failure surface at source areas is 44°. The sliding material did not always mobilize completely by flowing downslope. Debris flows travelled from a few meters up to more than 600 m, with differences in elevations (i.e. fall height) up to 230 m. In the latter settings, the total debris flow lengths measured are about 3.5 times greater than those occurred on terraced areas, with elevation differences up to 700 m. The striking difference in total length and elevation can be explained with the distribution of land use along the slopes, and with the different geomorphological settings. Nevertheless, an important factor governing the downslope debris flow evolution is the consistence of water supply at source areas. Debris flows are confined laterally where natural channels are present; otherwise they progressively increase in width along the slopes, up to 65m. As a consequence, small initial slides can affect wide portions of the slopes. Debris flows partially or totally destroyed retaining walls along their downslope path, eroding the superficial deposits and scraping off the vegetation. Usually the depth of erosion is limited to few decimeters, but values up to 2.5m have been measured. Deepening and washing out of materials along the axial part of landslides have been induced by superficial runoff or from water flowing from temporary springs located at source areas. Debris flows accumulation occurred on less steep reaches along the slopes, as morphologic terraces or roads, or at their foot, where the terrain gradient is less than 10°.

Slope failures occurred in glacial, fluvio-glacial, colluvial and anthropically reworked deposits. In most cases failure surfaces are localized at the boundary between horizons with different physical characteristics.

Available data of the area

- Topographic data
- Historical data (databases)
- Landslide inventory maps
- Digital Elevation Model
- Geological survey at municipality level
- Meteorological data (RICLIC Project)
- Thematic maps (preliminary analysis)
- Census data (ISTAT, Italian Institute of Statistics)

### **7.2.1) Selvetta debris flow**

On Sunday morning of 13<sup>th</sup> July 2008, after more than two days of intense rainfall (Figure 17), several debris and mud flows were released in the central part of Valtellina between Morbegno and Berbenno (Figure 18). One of the largest muddy-debris flows occurred in Selvetta, a fraction of Colorina municipality. According to the information from Civil Protection of Lombardy and interviews with local people, the flow occurred between 10:06 and 10:15 in the morning. The debris flow event was reconstructed after extensive field work and interviews with local inhabitants and civil protection teams. At

first several rock blocks of a size of almost 2 m<sup>3</sup> fell down from the direction of a small torrent. The blocks were followed by a second wave of debris and mud that destroyed completely one building and caused damages to other nine houses. There could be distinguished also a third wave of fine mud with high water content that partially washed away the accumulation from the second wave. Geomorphologic investigations allow distinguishing five main sections of the flow: 1) the proper scarp; 2) path in forested area; 3) path on alpine meadows; 4) accelerating section; 5) accumulation area. Initiation area of the flow is situated at 1760 m a.s.l. in a coniferous forest. The proper scarp is very small with an area of about 20 sq. m and height about 0.5 m. After some tens of meters the flow larger and denudated the channel of the torrent to the bedrock. The denudation of the channel to the bedrock is tightly associated with acceleration of the flow on steeper slope and rock steps. The Average inclination of the path in forested area is 35° but there are several steps with inclination higher than 60m. At 760 m a.s.l. the flow has decreased its velocity when reached less steep part of alpine meadows on morainic sediments near Rodolo village. The flow channel in this section of the flow is rarely denuded to the bedrock and flow itself accumulated a lot of material from the upper section. The average inclination of the third section is 24°. At the height of around 640 m a.s.l. the flow did not follow the original channel of Rodolo torrent and diverged more to the right side where joined a small ravine. The fourth part of the flow has an inclination about 34° and could be characterized with significant increase of velocity and denudation of the channel. At 310 m a.s.l. starts the apex of the accumulation zone. The volume of the debris was estimated by field mapping to be around 15 000 m<sup>3</sup> (Figure 19). Erosion and entrainment played an important role in the development of the debris flow. The precipitation records show that the initial failure did not occur immediately after the peak precipitation but about 2 hours later.

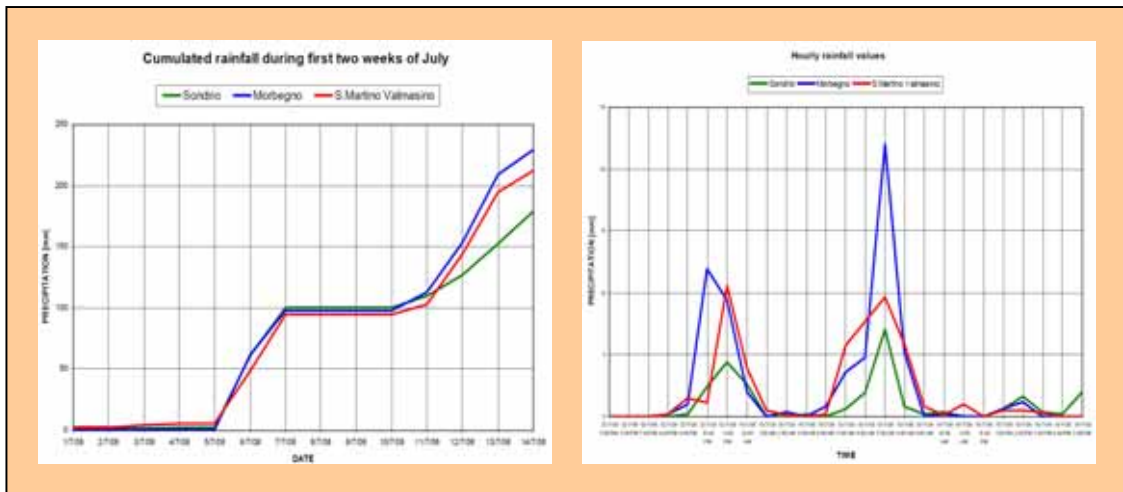


**Figure 17.** Cumulative rainfall before the Selvetta debris flow (left) and hourly rainfall values measured before the Selvetta event (right).



**Figure 18.** View of the Selvetta debris flow (left). View of the deposits and damage of the event (right)

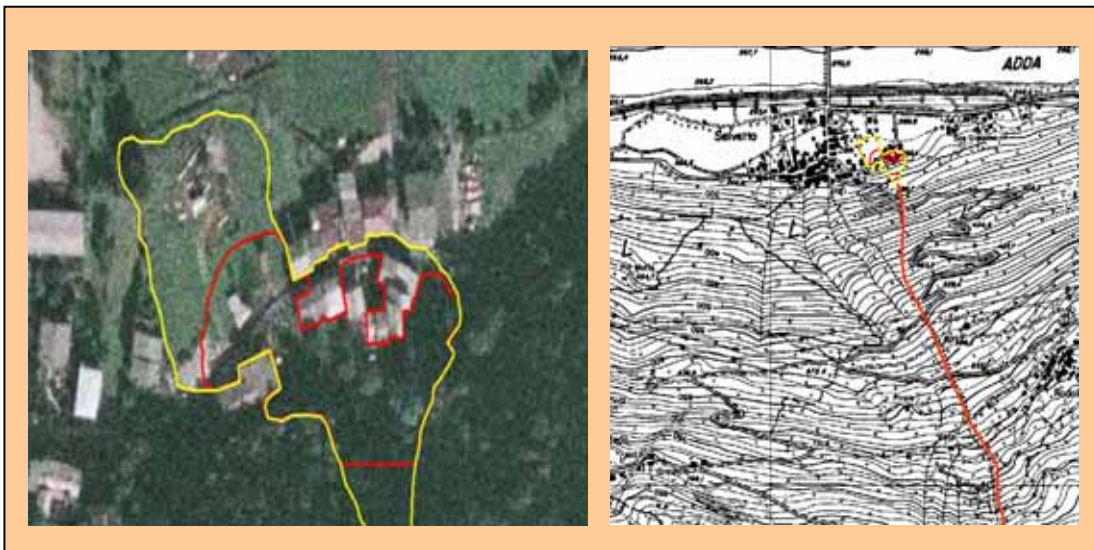


**Figure 19.** Aerial view of the Selvetta debris flow deposits (left). Contour map containing the trajectory of the Selvetta flow (right).

## 8) EGU abstracts accepted and future papers

### 8.1) Modelling the runout of a debris flow of the Western Ghats, Kerala, India

Sekhar L. Kuriakose (1), Byron Quan Luna (1), Santiago Begueria Portugues (2), C. J van Westen (1)

1. UNU-ITC School for Disaster Geo-information Management/Department of Earth Systems Analysis, International Institute for Geoinformation Science and Earth Observation (ITC), Enschede, The Netherlands (lukose11753@itc.nl, westen@itc.nl, quanluna@itc.nl / Fax: +31 53 4874336 / Phone: +31 53 4874263)
2. Estación Experimental de Aula Dei - Consejo Superior de Investigaciones Científicas (CSIC), (Aula Dei Experimental Station - Spanish National Research Council), Avda. Montañana 1005; 50059 - Zaragoza, Spain (sbegueria@eead.csic.es / Phone: +34 976 716107)

Debris flows as a result of shallow landslides are increasingly a concern in Kerala, the south western state of India. The plateau margins of highland Kerala (The Western Ghats) have all prerequisites of an active erosion zone where the natural terrain setup is conducive to slope failure/mass movements. Rainfall during two monsoons (South West and North East) that are effective in the state is identified as the primary trigger of debris flows. The flows are confined to the existing drainage lines and widen the streambeds that they follow, causing significant crop destruction (and occasionally loss of lives) along the path. Most often the amount of material that initiates the flows is less than a 1000 m<sup>3</sup>. Scouring is seen along the runout zone adding often an additional 30 to 80% more material.

One such debris flow event of 2001 which occurred in the Kottayam district of Kerala was modelled with a Coulomb frictional and a Voellmy model in the DAN3D software. DAN3D is based on a Lagrangian formulation that discretises the flow in a number of particles representing bed-normal columns of flow. The values of the field variables for each particle are calculated at each time step using an interpolation technique based on Smoothed Particle Hydrodynamics (SPH). Bed entrainment was simulated after defining an entrainment zone, a maximum depth of supply material and the average growth or erosion rate.

Result of the modeling shows that shallow failures using frictional material overestimates the runout zone and velocities. The Voellmy model underestimate deposit thickness where spreading is dominant but the velocity is better fitted during the course of the flow. Entrainment of material from the path and the ability to change rheology depending on the path material can be important. The reasonable results of the modeling show its flexibility which can be used to predict a simplified behaviour of debris flows.

## **8.2) Analysis of debris flow characteristics with a simple model incorporating entrainment processes.**

B. Quan Luna (1), A. Remaître (2), Th. W.J. van Asch (3), and J.-P. Malet (2)

(1) International Institute for Geo-Information Science and Earth Observation, Enschede, The Netherlands (quanluna@itc.nl),

(2) CNRS - University of Strasbourg, School and Observatory of Earth Sciences, Strasbourg, France, (3) Utrecht University, Faculty of Geosciences, Utrecht, The Netherlands

Entrainment of channel path material, and material deposition during run-out are key features of many rapid landslides like debris flows. Such mechanisms are able to change significantly the mobility of the flow, through rapid changes of the flow volume and of its rheology. Models using both a constant rheology and a constant volume cannot yield accurate forecast of debris-flows characteristics (velocity, discharge, flow height, spreading area), especially for debris flows occurring in heterogeneous torrential watersheds characterized by various geological settings and surficial deposits.

The objective of this paper is to present and test a simple 1D debris-flow model with a material entrainment concept based on limit equilibrium considerations and the generation of excess pore water pressure through undrained loading of the in situ material. The debris flow model propagation is based on a one dimensional finite difference solution of a depth-averaged form of the Navier-Stokes equations of fluid motions. The flows are treated as a one phase material, which behaviour is controlled by different rheological characteristics depending on the liquid/solid ratio. In this model, users are able to implement a change in rheology at the onset of entrainment. The model is tested on a debris flow event that occurred in 2003 in the Faucon torrent, and for which a detailed database on the sediment budget per reaches is available.

### **8.3) Debris flow reconstruction - geomorphologic and numerical approach. A case study from the Selvetta event in Valtellina, Italy, July 2008**

J. Blahut (1,2), B. Quan Luna (3), S. O. Akbas (1,2), and C. J. van Westen (3)

(1) Department of Environmental and Territorial Sciences, University of Milano-Bicocca, (DISAT-UNIMIB) Piazza della

Scienza 1, 20126 Milan, Italy, (2) Institute for the Dynamic Environmental Processes, National Research Council

(CNR-IDPA), Piazza della Scienza 1, 20126 Milan, Italy, (3) International Institute for Geoinformation Science and Earth

Observation (ITC), ITC, P.O. Box 6, 7500 AA Enschede, The Netherlands

On Sunday morning of 13th July 2008, after more than two days of intense rainfall, several debris and mud flows were released in the central part of Valtellina valley between Morbegno and Berbenno. One of the largest debris flows occurred in Selvetta, a fraction of Colorina municipality. The debris flow event was reconstructed after extensive field work and interviews with local inhabitants and civil protection teams. At first several rock blocks about 2 m<sup>3</sup> in size fell down from the direction of the torrent. The blocks were followed by a wave of debris and mud that immediately destroyed one building and caused damage to other nine houses. A stream flow following the debris flow consisting of fine mud with high water content that partially washed away the accumulation of deposits from the debris phase could also be distinguished. Geomorphologic investigations allowed identification of five main sections of the flow: 1) the proper scarp; 2) path in the forested area; 3) path on the alpine meadows; 4) accelerating section; 5) accumulation area. The initiation area of the flow is situated at 1760 m. a.s.l. (1480 m above the deposition zone) in a coniferous forest. The proper scarp consisted of an area of approximately 20 m<sup>2</sup> in size, and a height of about 0.8 m. The final volume of the debris was estimated by field mapping to be between 12 000 and 15 000 m<sup>3</sup>. It was observed that erosion and entrainment played an important role in the development of the debris flow. The Selvetta event was modelled with the FLO2D program. FLO2D is an Eulerian formulation with a finite differences numerical scheme that requires the specification of an input hydrograph. The internal stresses are isotropic and the basal shear stresses are calculated using a quadratic model. Entrainment was modeled at each section of the flow, and different hydrographs were produced in agreement with the behavior of the debris flow during its course. The significance of calculated values of pressure and velocity were investigated in terms of the resulting damage to the affected buildings. The physical damage was quantified for each affected structure within the context of physical vulnerability, which is defined as the ratio between the monetary loss and the reconstruction value. Two different empirical vulnerability curves were obtained, which are functions of debris flow velocity and pressure, respectively.

## **8.4) Estimation of Vulnerability Functions for Debris Flows Using Different Intensity Parameters**

S. O. Akbas (1,2), J. Blahut (1,2), B. Q. Luna (3), and S. Sterlacchini (2)

(1) Department of Environmental and Territorial Sciences, University of Milano-Bicocca, (DISAT-UNIMIB) Piazza della

Scienza 1, 20126 Milan, Italy., (2) Institute for the Dynamic Environmental Processes, National Research Council

(CNR-IDPA), Piazza della Scienza 1, 20126 Milan, Italy, (3) International Institute for Geoinformation Science and Earth

Observation (ITC), ITC, P.O. Box 6, 7500 AA Enschede, The Netherlands.

In landslide risk research, the majority of past studies have focused on hazard analysis, with only few targeting the concept of vulnerability. When debris flows are considered, there is no consensus or even modest agreement on a generalized methodology to estimate physical vulnerability of the affected buildings. Very few quantitative relationships have been proposed between intensities and vulnerability values. More importantly, in most of the existing relationships, information on process intensity is often missing or only described semi-quantitatively. However, robust assessment of vulnerabilities along with the associated uncertainties is of utmost importance from a quantitative risk analysis point of view. On the morning of 13th July 2008, after more than two days of intense rainfall, several debris and mud flows were released in the central part of Valtellina, an Italian alpine valley in Lombardy Region. One of the largest muddy-debris flows occurred in Selvetta, a fraction of Colorina municipality. The result was the complete destruction of two buildings, and damage at varying severity levels to eight others. The authors had the chance to gather detailed information about the event, by conducting extensive field work and interviews with local inhabitants, civil protection teams, and officials. In addition to the data gathered from the field studies, the main characteristics of the debris flow have been estimated using numerical and empirical approaches. The extensive data obtained from Selvetta event gave an opportunity to develop three separate empirical vulnerability curves, which are functions of deposition height, debris flow velocity, and pressure, respectively. Deposition heights were directly obtained from field surveys, whereas the velocity and pressure values were back-calculated using the finite difference program FLO2D. The vulnerability was defined as the ratio between the monetary loss and the reconstruction value. The monetary losses were obtained from official RASDA documents, which were compiled for claim purposes. For each building, the approximate reconstruction value was calculated according to the building type and size, using the official data given in the Housing Prices Index prepared by the Engineers and Architects of Milan. The resulting vulnerability curves were compared to those in the literature, and among themselves. Specific recommendations were given regarding the most suitable parameter to be used for characterizing the intensity of debris flows within the context of physical vulnerability.

## **8.5) The 4 January, 2009, landslide at "Los Chorros" village, San Cristóbal, Verapaz, Guatemala: context and a preliminary assessment**

J Cepeda (1), O. Hungr (2), B. Quan Luna (3), O.G. Flores Beltetón (4), M. Barillas (5), M.A. Mota Chavarría (6), J.R. Girón Mazariego (7), G. Devoli (8), S.E. Lauritzen (9), and M. Christen (10)

(1) International Centre for Geohazards, Norway ([jose.cepeda@geohazards.no](mailto:jose.cepeda@geohazards.no)), (2) University of British Columbia, Canada ([ohungr@eos.ubc.ca](mailto:ohungr@eos.ubc.ca)), (3) International Institute for Geoinformation Science and Earth Observation (ITC), The Netherlands ([quanluna@itc.nl](mailto:quanluna@itc.nl)), (4) Universidad de San Carlos de Guatemala, Guatemala ([omar\\_floresb@yahoo.com](mailto:omar_floresb@yahoo.com)), (5) Oxfam Great Britain, Guatemala ([embarillas@intelnet.net.gt](mailto:embarillas@intelnet.net.gt)), (6) Engineering geology consultant, Guatemala ([mmota\\_gt@yahoo.com](mailto:mmota_gt@yahoo.com)), (7) Instituto Nacional de Sismología, Vulcanología, Meteorología e Hidrología (INSIVUMEH), Guatemala ([jorgg17@yahoo.com](mailto:jorgg17@yahoo.com)), (8) Norwegian Geotechnical Institute (NGI), Norway ([gde@ngi.no](mailto:gde@ngi.no)), (9) Bergen University, Norway ([Stein.Lauritzen@geo.uib.no](mailto:Stein.Lauritzen@geo.uib.no)), (10) WSL Institute for Snow and Avalanche Research SLF, Switzerland ([christen@slf.ch](mailto:christen@slf.ch))

On 4 January, 2009, more than 5 million cubic metres of limestone and calcareous breccias detached from the "Los Chorros" hill and travelled along a tributary ravine of the Chixoy river in the municipality of San Cristóbal Verapaz, department of Alta Verapaz, Guatemala. At the time of this landslide, several persons were crossing roads and foot trails downstream of the release area. As of 14 January, authorities had reported 38 casualties, 50 missing and 5 injured persons. Along the landslide path, a 1.2 km segment of the 7W National Highway was destroyed, cutting the sole access route between San Cristóbal Verapaz and the western department of Quiché where numerous inhabitants of Alta Verapaz commute to work, especially during the coffee harvest season from October to March (with its peak on January). In response to this disaster, the Guatemalan government established four priorities: search and rescue activities, relief aid to victims and their families, evacuation of villages at risk and selection and construction of a temporary access route and a permanent road. In an attempt to provide additional elements to decision-makers of the Guatemalan authorities, this report is aimed to characterise the context of this landslide from a geosciences perspective. Preliminary assessments of the 4 January event and of other potentially unstable zones identified in the surrounding areas are also performed. The first accounts of ground instabilities in this area date back to 1590 when a 4.0 MS earthquake was associated with the collapse of a karst cave. In 1881, a Guatemalan newspaper reported that the San Cristóbal (Chichoj) lagoon was created after a ground subsidence was triggered by an earthquake. In 1983, after less than one year of operations, a 50 m segment of the 26-km long pressure tunnel in the Chixoy hydro electrical project was damaged due to an anhydrite karst produced during tunnel operations. In response to this event, repair and strengthening works were

carried out and power plant operation was re-started in 1985. At the end of November 2008, small landslides occurred in the surroundings of the area of the 4 January event and on mid December, a few number of larger slides occurred killing 2 persons and blocking the 7W National Highway. Rumbling noise was often reported by passersby. No heavy rainfall seems to be associated with the triggering of these events and rainfall accumulations during November 2008 (transition from rainy to dry season) were below the monthly normal rainfall. Immediately prior to these landslides, there are no earthquake events located in this area by the Guatemalan seismic network. During November 2008, three cold fronts affected Guatemala, producing freezing temperatures in some locations especially during the third week of November. In the surroundings of the area of the 4 January landslide, frost susceptibility ranges from low to medium. The landslide took place in a catchment that follows a NNE fault which to the south intersects the EW Chixoy-Polochic fault (part of the transcurrent boundary of the North American and the Caribbean plates) 5 km downstream of the release area. Some fumarolic activity is currently observed in the landslide site. Based on the above elements and on observations from field reconnaissance missions, some hypotheses are formulated to explain the conditioning and triggering factors for the events in November and December and particularly for the 4 January landslide. These hypotheses are aimed to help to identify other potential instabilities in the surroundings.

Back-calculation of flow parameters for the 4 January landslide has been possible based on estimation of velocities using video footage of the event and simulations with two different models for landslide dynamics across three-dimensional terrain: DAN3D developed at the University of British Columbia and RAMMS developed at the WSL Institute for Snow and Avalanche Research SLF. These back-calculated parameters have enabled the estimation of impact areas due to landslides that can be potentially released in surrounding slopes with similar instability features to the “Los Chorros” hill. Even though these estimations may be improved as more information becomes available for this event, the authors hope that this report contributes with some elements for decision-makers regarding short- and intermediate-term activities in response to this disaster.

## **9) Future collaborations**

- Theo van Asch (Utrecht University)
- Karim Kelfour (University Blais Pascal, Clermont)
- Alexander Remaitre and Jean Phillippe Malet (Strasbourg)
- Santiago Beguerria (Zaragoza)
- Michel Jaboyedoff (Lausanne)
- Gianluca Marcato (CNR Italy)
- Marc Christensen (SLF DAVOS)
- Margareth Keller (Vienna)
- Dieter Issler (snow) and Kalle Kronholm (hazard mapping) (NGI)
- University of Milan

## 10) References

- P. Aleotti and R. Chowdhury, Landslide hazard assessment: summary review and new perspectives. – *Bull. Eng. Geol. Environ.*, 58, (1999) pp. 21-44.
- M. Barbolini, F. Cappabianca and R. Sailer, Empirical estimate of vulnerability relations for use in snow avalanche risk assessment. In: C.A. Brebbia, Editor, Proceedings of the 4th International Conference on Computer Simulation in Risk Analysis and Hazard Mitigation “Risk Analysis 2004”, 27–29 September, Rhodes, Greece, WIT Press (2004), pp. 533–542.
- C. Bonnard, F. Forlati and C. Scavia. Identification and mitigation of large landslide risks in Europe. Advances in risk assessment. – Balkema, Leiden, (2003) 317p.
- S.H. Cannon and W.Z. Savage , A mass change model for debris flow. *The Journal of Geology* 96 (1988), pp. 221–227.
- A Carrara, M. Cardinali, R. Detti, F. Guzzetti, V. Pasqui and P. Reichenbach, GIS techniques and statistical models in evaluating landslide hazard. – *Earth Surf. Proc. & Landforms*, 16, (1991) pp.427-445.
- C.L. Chen, Comprehensive review of debris flow modeling concepts in Japan. – *Geol. Soc. Am. Rev. Eng. Geol.*, 7, (1987) pp. 13-29.
- H. Chen and C.F. Lee , Numerical simulation of debris flows. *Canadian Geotechnical Journal* 37 (2000), pp. 146–160.
- H. Chen and C.F. Lee, A dynamic model for rainfall induced landslides on natural slopes. – *Geomorphology*, 51, (2003) pp. 269-288.
- J.A. Coe, J.W. Godt, M. Parise, and A. Moscariello, Estimating debris flow probability using debris-fan stratigraphy, historic records, and drainage-basin morphology, Interstate 70 Highway Corridor, Central Colorado. In : *Proc. 3rd Int. Conf. on Debris-flow hazards mitigation : mechanics, prediction and assessment*, Davos, Switzerland. – Millpress, Rotterdam, (2003) pp. 1085-1096.
- J.A. Coe, J.A. Michael, R.A. Crovelli, W.Z. Savage, W.T. Laprade and W.D. Nashem, Probabilistic assessment of precipitation triggered landslides using historical records of landslide occurrence, Seattle, Washington. – *Environ. Eng. Geoscience*, 10, (2004) 103-122.
- J. Corominas , The angle of reach as a mobility index for small and large landslides. *Canadian Geotechnical Journal* 33 (1996), pp. 260–271.

- D.M. Cruden , A simple definition of a landslide. *Bulletin of the International Association of Engineering Geology* 43 (1991), pp. 27–29.
- T.R. Davies, M.J. McSaveney and K.A. Hodgson, A fragmentation-spreading model for long-run-out rock avalanches. – *Can. Geotech. J.*, 36, (1999) pp. 1096-1110.
- R.P Denlinger and R.M Iverson, Granular avalanches across irregular three-dimensional terrain; 1. Theory and computation. – *J. Geophys. Res.*, 109, F01014. (2004)
- W.E. Dietrich, D. Bellugi and R. Real de Asua, Validation of the shallow landslide model, SHALSTAB, for forest management. *In: Landuse and watersheds : human influence on hydrology and geomorphology in urban and forest areas.* – AGU, *Water Science and Applications*, 2, (2001) pp.195-227.
- A.G. Fabbri and C.J. Chung, Predictive spatial data analyses in the geosciences. *In: Spatial analytical perspectives on GIS in the environmental and socio-economic sciences; GISDATA 3* – Taylor & Francis, London, (1996) pp.147-159.
- R. Fell and D. Hartford , Landslide risk management. *In: D. Cruden and R. Fell, Editors, Landslide Risk Assessment*, Balkema, Rotterdam (1997), pp. 51–109.
- P.J. Finlay, P.R. Mostyn and R. Fell, Landslide risk assessment: prediction of travel distance. – *Can. Geotech. J.*, 36, (1999) pp. 556-562.
- R.W. Fleming, S.D. Ellen and M.A. Albus , Transformation of dilative and contractive landslide debris into debris flows—an example from Marin County, California. *Engineering Geology* 27 (1989), pp. 201–223.
- J.L Garcia, J.L. Lopez, M. Noya, M.E. Bello, M.T. Bello, N. Gonzales, G. Paredes and M.I. Vivas, Hazard mapping for debris flow events in the alluvial fans of northern Venezuela. *In: Proc. 3rd Int. Conf. on Debris-Flow Hazards Mitigation: Mechanics, Prediction and Assessment*, Davos, Switzerland. – Millpress, Rotterdam, (2003) pp. 589-600.
- T. Glade, P. Albini, F. Frances, The use of historical data in natural hazard assessments. – *Advances of Technological and Natural Hazard Research*, Kluwer, Rotterdam, (2001) p.220
- N.F. Glenn, D.R. Streutker, D.J. Chadwick, G.D. Thackray and S.J. Dorsch, Analysis of LiDAR-derived topographic information for characterizing and differentiating landslide morphology and activity. – *Geomorphology.*, 73, (2006) pp.131-148.
- J.M.N.T. Gray, M. Weiland, K. Hutter, Gravity-driven free surface flow of granular avalanches over complex basal topography. – *Proc., Royal. Soc. London, Ser. A.*, 455, (1999) pp. 1841-1874.

- R.H. Guthrie and S.G. Evans, The role of magnitude-frequency relations in regional landslide risk analysis. *In: Proc. Int. Conf. on Landslide risk management*, Vancouver, Canada. – Balkema, Leiden, (2005) pp. 375-380.
- F. Guzzetti, A. Carrara, M. Cardinali and P. Reichenbach, Landslide hazard evaluation: a review of current techniques and their application in a multi-scale study, Central Italy. – *Geomorphology*, 31, (1999) pp. 181-216.
- C. Harbitz. Snow avalanche modelling, mapping and warning in Europe. Deliverable No. 4. A survey of computational models for snow avalanche motion. Oslo, Norwegian Geotechnical Institute. (NGI Technical Report 581220-1. (1999)
- G. Hunter and R. Fell, Travel distance angle for rapid landslides in constructed and natural soil slopes. – *Can. Geotech. J.*, 40, (2003) pp.1123-1141.
- K. Ho, E. Leroi and B. Roberts , Keynote lecture: quantitative risk assessment—application, myths and future direction. In: *Proceedings of the International Conference on Geotechnical and Geological Engineering, GEOENG 2000*, Melbourne, Australia vol. 1, Technomic, Lancaster (2000), pp. 236–312.
- J.P. His and R. Fell, Landslide risk assessment of coal refuse emplacement. *In: Proc. Int. Conf. on Landslide risk management*, Vancouver, Canada. – Balkema, Leiden, (2005) pp.525-532.
- O. Hungr, G.C. Morgan and R. Kellerhals, Quantitative analysis of debris torrent hazards for design of remedial measures. – *Can. Geotech. J.*, 21, (1984) pp.663-667.
- O. Hungr , A model for the runout analysis of rapid flow slides, debris flows, and avalanches. *Canadian Geotechnical Journal* 32 (1995), pp. 610–623.
- O. Hungr and S.G. Evans, Entrainment of debris in rock avalanches : An analysis of a long run-out mechanism. – *Geol. Soc. Amer. Bull.*, 116, (2004) pp. 1240-1252.
- O. Hungr, J. Corominas, E. Eberhardt, Estimating landslide motion mechanism, travel distance and velocity. *In: Proc. Int. Conf. on Landslide risk management*, Vancouver, Canada. – Balkema, Leiden, (2005) pp. 99-128.
- J.N. Hutchinson , A sliding-consolidation model for flow slides. *Canadian Geotechnical Journal* 23 (1986), pp. 115–126
- K. Hutter, T. Kocht, C. Pluss and S.B. Savage, The dynamics of avalanches and granular material from initiation to run-out. Part II. Experiments. – *Acta Mechanica*, 109, (1995) pp. 127-165.
- R.M. Iverson, The physics of debris flows. – *Rev. Geophys.*, 35, (1997) pp. 245-296.

- R.M. Iverson, M. Logan and R.P. Denlinger, Granular avalanches across irregular three-dimensional terrain. 2: Experimental tests. – *J. Geophys. Res.*, 109, F01015. (2004)
- R.M. Iverson, Debris flow mechanics. *In* : Debris flows and related phenomena. – Praxis, Chichester, (2005) 36-51.
- M. Jakob, D. Anderson, T. Fuller, O. Hungr and D. Ayotte, An unusually large debris flow at Hummingbird Creek, Mara Lake, British Columbia. – *Can. Geotech. J.*, 37, (2000) pp. 1109-1125.
- K. Jónasson, S. Sigurðson and Þ. Arnalds, Estimation of avalanche risk, Vedurstofu Islands n. R99001-UR01 (1999) 44 pp..
- A.M. Johnson and J. R. Rodine, Debris flow. *In*: Slope instability. – Wiley, Chichester, (1984) pp.257-361
- C.J. Keylock and M. Barbolini, Snow avalanche impact pressure — vulnerability relations for use in risk assessment, *Canadian Geotechnical Journal* 38 (2001), pp. 227–238.
- D. Laigle and P. Coussot , Numerical modelling of mudflows. – *ASCE J. Geotech. Eng.*, 123, (1997) pp. 617-623
- D. Laigle, A.F. Hector, J. Hubl and D. Rickenmann, Comparison of numerical simulation of muddy debris flow spreading to records of real events. *In*: Proc. 3rd Int. Conf. on Debris-flow hazards mitigation : mechanics, prediction and assessment, Davos, Switzerland. – Millpress, Rotterdam, (2003) pp.635-646
- E.M. Lee, J.W. Hall, I.C. Meadowcroft, Coastal cliff recession: the use of probabilistic prediction methods. – *Geomorphology.*, 40, (2001) pp. 253-269.
- M. Lehning, P. Bartelt,, R.L Brown, T. Russi, U. Stöckli, M. Zimmerli, Snowpack Model Calculations for Avalanche Warning based upon a new Network of Weather and Snow Stations, *Cold Reg. Sci. Technol.*, 30, (1999) pp.145-157.
- S. Leroueil and J. Locat , Slope movements—geotechnical characterization, risk assessment and mitigation. *In*: B. Maric, L. Lisac and A. Szavits-Nossan, Editors, Geotechnical Hazards, Balkema, Rotterdam (1998), pp. 95–106.
- S. Leroueil, J. Locat, J. Vaunat, L. Picarelli, H. Lee and R. Faure , Geotechnical characterization of slope movements. *In*: K. Senneset, Editor, Landslides, Balkema, Rotterdam (1996), pp. 53–74.
- K. Lied and S. Bakkehoi, Empirical Calculations of Snow Avalanche Run-out Distance Based on Topographic Parameters. *Journal of Glaciology*, 26(94):165-177, (1980).

- J. Locat, Normalized rheological behaviour of fine muds and their flow properties in a pseudoplastic regime. *In: Proc. 1st Int. Conf. on Debris-flow hazards mitigation: mechanics, prediction and assessment*, San Francisco, U.S. America – ASCE, New-York, (1997) pp. 260-269.
- J.P. Malet and S. Begueria-Protugues, Probabilistic assessment of debris flow hazard on alluvial fans. – (submitted) (2007).
- A. Mangeney-Castelnaud, J.P. Vilotte, O. Bristeau, B. Perthame, F. Bouchut, C.Simeoni, and S. Yeremi, Numerical modeling of avalanches based on Saint-Venant equations using a kinetic scheme. – *J. Geophys. Res.*, 108, (2003) p.2527.
- S. McDougall and O. Hungr, A universal model for 3-D run-out analysis of landslides. *In: Landslides evaluation & stabilization, Proc. 9th Int. Symp. on Landslides*, Rio de Janeiro, Brazil. – Balkema, Leiden, (2004) pp. 1485-1488.
- G.C. Morgan, G.E. Rawlings and J.C. Sobkowicz, Evaluating total risk to communities from large debris flows. *In: Proceedings of 1st Canadian Symposium on Geotechnique and Natural Hazards*, BiTech Publishers, Vancouver, BC, Canada (1992), pp. 225–236.
- G.R. Mostyn and R. Fell, Quantitative and semiquantitative estimation of the probability of landsliding. *In: D. Cruden and R. Fell, Editors, Landslide Risk Assessment*, Balkema, Rotterdam (1997), pp. 297–315.
- J. S. O'Brien, P.Y. Julien and W.T. Fullerton, Two-dimensional water flood and mudflow simulation. – *J. Hydr. Eng.*, 119, (1993) pp. 224-261.
- M. Pirulli, Numerical modelling of landslide runout: A continuum mechanics approach. – Ph.D. Thesis, Politecnico di Torino, Italy, (2005)
- A. Remaitre, J.P. Malet, O. Maquaire, Morphology and sedimentology of a complex debris flow in a clay-shale basin. *Earth Surf. Process. Landforms* 30 (2005) pp.339-348.
- A. Remaitre, J.P. Malet, O. Maquaire, Flow behaviour and runout modelling of complex debris flow in a clay-shale basin. *Earth Surf. Process. Landforms* 30 (2005) pp.479-488.
- B. Salm, A Short and Personal History of Snow Avalanche Dynamics. *Cold Region Science and Technology*, 39: (2004) pp. 83-92
- K. Sassa, Geotechnical model for the motion of landslides. *In: C. Bonnard, Editor, Proceedings of 5th International Symposium on Landslides*, Lausanne, Balkema, Rotterdam (1988), pp. 37–55.
- W.Z. Savage, J.W. Godt, R.L. Baum, A model for spatially and temporally distributed shallow landslide initiation by rainfall infiltration. *In: Proc. 3rd Int. Conf. on Debris-flow*

*hazards mitigation : mechanics, prediction and assessment*, Davos, Switzerland. – Millpress, Rotterdam, (2003) pp. 179-187.

- S.B. Savage and K. Hutter, The dynamics of avalanches and granular material from initiation to run-out. Part I : Analysis. – *Acta Mech.*, 86, (1991) pp. 201-223.

- A. Scheidegger, On the prediction of the reach and velocity of catastrophic landslides. – *Rock Mech.*, 5, (1973) pp. 231-236.

- R. Soeters and C.J. van Westen , Slope instability, recognition, analysis, and zonation. In: A.K. Turner and R.L. Schuster, Editors, *Landslides: Investigation and Mitigation*, Special Report 247, Transportation Research Board, National Research Council, National Academy Press, Washington, DC (1996), pp. 129–177

- J. Soussa and B. Voight, Continuum simulation of flow failures. – *Geotechnique*, 41, (1991) pp. 515-538.

- T. Takahashi, Debris flows. – IAHR Publication, Balkema, Rotterdam, (1991) p.231

- C.J. van Westen, N. Rengers, M.T.J. Terlien and R. Soeters , Prediction of the occurrence of slope instability phenomena through GIS-based hazard zonation. *Geologische Rundschau* 86 (1997), pp. 404–414

- C.J. van Westen, Th. W.J van Asch and R. Soeters, Landslide hazard and risk zonation - why is it still so difficult? – *Bull. Eng.Geol. Env.*, 65, (2006) pp. 167-184.

- L. Vulliet, Three families of models to predict slowly moving landslides. *In: Computer methods and advances in geomechanics*. – Balkema, Rotterdam, (1997) pp. 277-284.

- L. Vulliet, Natural slopes in slow movement. *In: Modeling in geomechanics*. – Wiley & Sons, Chichester, (2000) pp. 653-676.

- G. Wang and K. Sassa, Pore pressure generation and movement of rainfall-induced landslides: effects of grain size and fine particle content. – *Eng. Geol.*, 69, (2003) pp. 109-125.

- G.F. Wieczorek , Preparing a detailed landslide-inventory map for hazard evaluation and reduction. *Bulletin of the Association of Engineering Geologists* 21 3 (1984), pp. 337–342.

- C. Wilhelm, Quantitative risk analysis for evaluation of avalanche protection projects. In: E. Hestness, Editor, *Proc. of 25 Years of Snow Avalanche Research*, Voss 12–16 May 1998,, NGI Publications vol. 203, Norway, Oslo (1998), pp. 288–293.

- N. Wong, Landslide risk assessment for individual facilities. *In: O. HUNGR, R. FELL, R. COUTURE & E. EBERHARDT, Eds., Proc. Int. Conf. on Landslide risk management, Vancouver, Canada. – Balkema, Leiden, (2005) pp. 237-296*

- T.H. Wu, W.H. Tang and H.H. Einstein , Landslide hazard and risk assessment. *In: A.K. Turner and R.L. Schuster, Editors, Landslides: Investigation and Mitigation, Special Report 247, Transportation Research Board, National Research Council, National Academy Press, Washington, DC (1996), pp. 106–*

## APPENDIX

### MassMov one dimensional vertical slices with scouring

The shear stress ( equation 1 ) and normal stress Equation 2) for calculating respectively the driving force and frictional resistance are given according to the scheme of Figure 1 as follows :

$$\text{weight slice} = \rho_{fl} gh * 1$$

$$\tau = \rho_{fl} gh \frac{\sin\alpha}{1/\cos\alpha} = \rho_{fl} gh \sin\alpha \cos\alpha \quad (1)$$

$$\sigma = \rho_{fl} gh \frac{\cos\alpha}{1/\cos\alpha} = \rho_{fl} gh \cos^2\alpha \quad (2)$$

$$\frac{\partial h}{\partial t} + \frac{\partial(hu)}{\partial x} = 0 \quad (\text{mass balance}) \quad (3)$$

$$\frac{\partial u}{\partial t} + u \frac{\partial u}{\partial x} = g \cos\alpha_x \left[ \sin\alpha_x \cos\alpha_x - k \frac{\partial h}{\partial x} - S_f \right] \quad (4a)$$

$$S_f = \left[ \cos^2\alpha_x \tan\phi' + \frac{1}{\rho h} \left( \tau_c + \eta \left( \frac{\partial u}{\partial z} \right)^b \right) \right] \quad (4b) \text{ Herschel Bulkley /Coulomb viscous}$$

Equation 3 is the mass balance equation ( u = velocity) while equation 4 at the left hand describes the balance between driving force (first term) , the pressure term ( second term) and the resistance forces ( third term) in terms of acceleration (L/T<sup>2</sup>). The inertial term is ignored for this slow moving landslides.

Equation 4 is the Herschel –Bulkley resistance term, which is chosen here. It is the Coulomb viscous resistance term when b=1

Going to a numeric solution of the above mentioned equations we can rewrite equation 3 and 4

$$Sf_i^n = \cos^2 \alpha_i \tan \varphi' + \frac{1}{\rho h_i^n} \left( \frac{3}{2} \tau_c + \frac{3\eta}{h_i^n} u_i^n \right)$$

$$u_i^{n+1/2} = \text{lax } u_i^n - \cos \alpha_i \frac{1/2 \Delta t}{s} u_i^n (u_{i+1}^n - u_{i-1}^n) + 1/2 \Delta t g \cos \alpha_i \left[ + (\sin \alpha_i \cos \alpha_i) - \frac{1}{s} k (h_{i+1}^n - h_{i-1}^n) - Sf_i^n \right]$$

( $\alpha$  positive downslope)

$$Sf_i^{n+1/2} = \cos^2 \alpha_i \tan \varphi' + \frac{1}{\rho h_i^n} \left( \frac{3}{2} \tau_c + \frac{3\eta}{h_i^n} u_i^{n+1/2} \right)$$

$$u_i^{n+1} = \text{lax } u_i^n - \cos \alpha_i \frac{\Delta t}{s} u_i^n (u_{i+1}^n - u_{i-1}^n) + \Delta t g \cos \alpha_i \left[ + (\sin \alpha_i \cos \alpha_i) - \frac{1}{s} k (h_{i+1}^n - h_{i-1}^n) - Sf_i^{n+1/2} \right]$$

$$h_i^{n+1} = \text{lax } h_i^n - \frac{\Delta t}{s} (u h_i^n - u h_{i-1}^n)$$

There are a lot of alternative descriptions for Sf depending on the rheology

Simple Bingham and Coulomb viscous:

$$Sf = g \frac{1}{\rho h} \left( \frac{3}{2} \tau_c + \frac{3\eta}{h} u \right)$$

$$Sf = g \left[ \cos^2 \alpha \tan \varphi' + \frac{1}{\rho h} \left( \frac{3}{2} \tau_c + \frac{3\eta}{h} u \right) \right]$$

Voellmy:

$$Sf = g \left[ \cos^2 \alpha \tan \varphi' + \frac{u^2}{\xi h} \right] \equiv g \left[ \cos^2 \alpha \tan \varphi' + \frac{u^2}{C^2 h} \right]$$

Quadratic

$$Sf = g \left[ \frac{\tau_c}{\rho h} + \frac{K\eta}{8\rho(h)^2} u + \frac{n^2(u)^2}{(h)^{2/5}} \right] \quad K = 24$$

Respectively Newton turbulent, Idem& Coulemb, Idem& Yield, Idem& Coulemb& Yield:

$$Sf = g \frac{u^2 n^2}{h^{4/3}}$$

$$Sf = g \left[ \frac{u^2 n^2}{h^{4/3}} + \cos^2 \alpha \tan \phi' \right]$$

$$Sf = g \left[ \frac{u^2 n^2}{h^{4/3}} + \frac{\tau_c}{\rho h} \right]$$

$$Sf = g \left[ \frac{u^2 n^2}{h^{4/3}} + \frac{\tau_i}{\rho h} \right]$$

$$\tau_i = \min(\tau_c, \rho g h \sin \alpha \cos \alpha \tan \phi')$$

Newton laminar can be extended with a Coulomb, Yield and Coulomb& Yield component (see above):

$$Sf = \frac{1}{\rho h} \left( \frac{3\eta}{h} u \right)$$

### **Scouring**

Increase in vertical load at underground when debris flow arrives *for slice i* (suffix i not mentioned anymore in equations below)

$$\Delta \sigma = \rho_{fl} g h \cos^2 \alpha$$

Increase in shear stress :

$$\Delta \tau = \rho_{fl} g h \sin \alpha \cos \alpha$$

This means an increase in pore pressure according to Skempton modified by Sassa

$$\Delta p = B_D (\Delta \sigma + A_D \Delta \tau)$$

The total vertical stress at the bottom of in situ material (hard rock) is then

$$\sigma_{tot} = (\rho_{fl} g h + \rho_{id} g d) \cos^2 \alpha$$

Idem shear stress:

$$\tau_{tot} = (\rho_{fl} g h + \rho_{id} g d) \sin \alpha \cos \alpha$$

May be there is groundwater flowing in the in situ material with height  $d_w$

$$p_{ini} = \rho_w g d_w \cos^2 \alpha$$

Then total pore pressure becomes:

$$p_{\text{tot}} = p_{\text{ini}} + \Delta p$$

The safety factor at the bottom of in situ material is then:

$$F_{\text{bottom}} = \frac{c_{\text{id}} + (\sigma_{\text{tot}} - p_{\text{tot}}) \tan \delta_{\text{id}}}{\tau_{\text{tot}}}$$

The safety factor at the surface ( boundary between in situ material and bottom debris flow) of the in situ material is then

$$F_{\text{top}} = \frac{c_{\text{id}} + (\Delta \sigma - \Delta p) \tan \delta_{\text{id}}}{\Delta \tau}$$

In case  $F_{\text{bottom}} > 1$  and  $F_{\text{top}} < 1$  calculate depth of failure ( $d_f$ ), which is the amount of material taken away (expressed as a vertical height)

$$d_f = \frac{1 - F_{\text{top}}}{F_{\text{bottom}} - F_{\text{top}}} d$$

In case  $F_{\text{bottom}} < 1$  all the material is taken away

Possible liquefaction if  $r_p > 1$

$$r_p = \frac{p_{\text{tot}}}{\sigma_{\text{tot}}}$$